*American Mineralogist, Volume 91, pages 1521–1535, 2006*

# The petrogenesis of the Apollo 14 high-Al mare basalts

**CLIVE R. NEAL* AND GEORGIANA Y. KRAMER**

Department of Civil Engineering and Geological Sciences, University of Notre Dame, Notre Dame, Indiana 46556, U.S.A.

## ABSTRACT

In this paper, we report analysis of various basaltic lunar samples including 14053 and 14072, KREEP basalt 15386, thirty basalt clasts from Apollo 14 breccia 14321, as well as impact-generated samples (matrix from breccia 14168, olivine vitrophyres 14321,1180 and 14321,1539, and impact melt 14310) using a combination of solution and laser ablation inductively coupled plasma mass spectrometry (ICP-MS). The basalt clast samples were previously analyzed by instrumental neutron activation. On plots of incompatible trace elements (ITEs) vs. compatible trace elements, the Apollo 14 high-Al basalts form three approximately subparallel trends that, on the basis of current data, are also separated by age. Plots of ITE ratios (i.e., Nb/Ce vs. Zr/Y) can be used to indicate source composition, and also divide the basalts into three groups: Group A (~4.3 Ga); Group B (~4.1 Ga); and Group C (~3.9 Ga). New data for 14072 suggest the sample does not fit with any of the three groups defined here, and may indicate the presence of a fourth group of high-Al basalts in the proximity of the Apollo 14 site. The Apollo 14 high-Al basalts are compositionally distinct from known Apollo 14 impact melts and impact-generated lithologies. The three groups cannot be related by varying degrees of partial melting of a single, KREEP-contaminated source and, therefore, require three separate source regions. The new data indicate that Group A basalts evolved through closed-system crystal fractionation. However, the new data from basalts forming Groups B and C require open-system evolution that involves combined assimilation and fractional crystallization (AFC). Unlike previous AFC modeling of the Apollo 14 high-Al basalts, an assimilant composed of KREEP is not sufficient to generate the compositional ranges of each basalt group. The modeling of both groups requires a mixture of KREEP and granite as the assimilant, which supports the notion of a genetic relationship between these two lunar components.

**Keywords:** Moon, assimilation, basalt petrogenesis, Apollo 14 high-Al basalts, mare basalts, fractional crystallization, KREEP, granite

## INTRODUCTION

The Apollo 14 mission landed in the Fra Mauro region of Oceanus Procellarum (Fig. 1) in February, 1971 and returned 42 kg of lunar samples that consisted of predominantly impact-generated breccias. Some of these breccias contained a wealth of basaltic clasts and these have proven to be significant because they are, at present, the only samples that record pre-4 Ga volcanism on the Moon (Taylor et al. 1983; Dasch et al. 1987). On the basis of current data, the basaltic clasts from the Fra Mauro region represent mare volcanic events that that occurred over a period of ~400 Myr from ~3.9 to ~4.3 Ga (Papanastassiou and Wasserburg 1971; Compston et al. 1971, 1972; Taylor et al. 1983; Dasch et al. 1987; Shih and Nyquist 1989a, 1989b). This age range pre-dates the main mare magmatism recorded at other sample return sites (e.g., Nyquist and Shih 1992; Snyder et al. 2000) and may represent the end of the effusive cryptomare eruptions (Head and Wilson 1992). In addition, the major-element geochemistry of the basalts is distinct relative to the great majority of mare basalts from other sample return sites. The Fra Mauro basalts are relatively enriched in $Al_2O_3$ (11–16 wt%) and hence, in a lunar reference, are termed "high-Al" (e.g., Ridley 1975). Samples returned by Luna 16 from Mare Fecunditatis are also high-Al, containing from 11 to ~19 wt% $Al_2O_3$ (e.g., Albee et al. 1972; Grieve et al. 1972; Helmke and Haskin 1972; Kurat et al. 1976; Ma et al. 1979), but are significantly younger (~3.4 Ga; Papanastassiou and Wasserburg 1972). The high-Al nature of both the Apollo 14 and Luna 16 basalts is manifest in the fact that they contain proportionally greater modal plagioclase relative to mare basalts from other sample return sites (e.g., Albee et al. 1972; Papike et al. 1974; Papike and Vaniman 1978; Neal and Taylor 1992).

The Fra Mauro region is generally accepted as being made up of ejecta deposits from the Imbrium impact (Wilhelms 1987). The Apollo 14 high-Al basalts, therefore, probably are not indigenous to that region. The surface flows from which the clasts were derived probably originated from the Imbrium region prior to basin formation. These units now either are covered by younger mare flows, have been effectively obliterated by subsequent impacts, and/or are masked by impact ejecta.

Although they show relatively small to moderate variations in major-element chemistry, the Apollo 14 high-Al basalts do exhibit a large range in trace-element abundances. Though using different nomenclature, both Shervais et al. (1985) and Dickinson et al. (1985) divided these basalts into groups on the basis of incompatible-trace-element (ITE) abundances (Fig. 2a). They noted a general increase in FeO and MgO as ITE abundances decrease, leading Dickinson et al. (1985) to conclude their more

* E-mail: neal.1@nd.edu

**Table 1.** Trace element data for samples analyzed in this study by ICP-MS. All values are in $\mu$g/g or parts per million (ppm)

| | BHVO-1[S] | 1δ | Ref. values[1] | BHVO-2[S] | 1δ | Ref. values[2] | NIST[L] 612 glass | 1δ | Ref. values[3] | 15386,48[S] KREEP basalt | Lit. values[4] | 14168,34[S] Breccia matrix |
|---|---|---|---|---|---|---|---|---|---|---|---|---|
| **Be** | 0.88 | 0.01 | 1.1 | 1.02 | 0.09 | | 47.6 | 14.5 | 37.7 | 5.81 | | 5.6 |
| **Sc** | 33.8 | 1.56 | 31.8 | 35.4 | 2.38 | 32 | NA | | | 24.8 | 23.6 | 32.3 |
| **V** | 331 | 50.4 | 317 | 310 | 71.8 | 317 | 39.3 | 1.3 | 39.2 | 52.1 | | 59.7 |
| **Cr** | 352 | 59.4 | 289 | 315 | 72.7 | 280 | 43 | 6.53 | 39.9 | 1954 | 2400 | 1757 |
| **Co** | 54 | 3.86 | 45 | 55.3 | 4.36 | 45 | 35.2 | 1.84 | 35.3 | 25.5 | 17.9 | 48.1 |
| **Ni** | 133 | 8.82 | 121 | 124.2 | 11.2 | 119 | NA | | | 14.8 | 12.5 | 405 |
| **Cu** | 183 | 66.5 | 136 | 145 | 15.7 | 127 | 34.8 | 6.6 | 36.71 | 16.7 | 3.5 | 20.4 |
| **Ga** | 23.8 | 3.44 | 21 | 22.2 | 2.27 | 21.7 | 36.3 | 1.82 | 36.2 | 5.18 | | 7.53 |
| **Rb** | 9.86 | 0.48 | 11 | 9.48 | 1 | 9.8 | 31.8 | 1.55 | 31.6 | 18.8 | 18.46 | 6.43 |
| **Sr** | 407 | 19.1 | 403 | 414 | 26.8 | 389 | 76.4 | 2.87 | 76.2 | 192 | 187.4 | 170 |
| **Y** | 25.2 | 1.81 | 27.6 | 24.9 | 1.23 | 26 | 38.4 | 1.56 | 38.3 | 248 | | 204 |
| **Zr** | 172 | 3.32 | 179 | 184 | 8.95 | 172 | 36.2 | 1.48 | 36 | 1050 | 970 | 999 |
| **Nb** | 19.8 | 0.44 | 19 | 20.1 | 1.74 | 18 | 38.1 | 1.77 | 38.1 | 80.2 | | 75.2 |
| **Mo** | 1.03 | 0.05 | 1.02 | 4.71 | 0.18 | | NA | | | 0.2 | | 0.2 |
| **Sn** | 2.06 | 0.05 | 2.1 | 1.99 | 0.16 | 1.9 | 37.9 | 2 | 38 | 0.03 | | 0.06 |
| **Sb** | 0.17 | 0.04 | 0.16 | 0.24 | 0.02 | | 38.5 | 2.17 | 38.4 | 0.03 | | 0.03 |
| **Cs** | 0.07 | 0.02 | 0.13 | 0.08 | 0.004 | | 41.7 | 2.21 | 41.6 | 0.77 | | 0.24 |
| **Ba** | 137 | 1.88 | 139 | 135 | 1.89 | 130 | 37.9 | 1.48 | 37.7 | 863 | 837 | 780 |
| **La** | 15.9 | 0.37 | 15.8 | 15.5 | 0.32 | 15 | 35.9 | 1.35 | 35.8 | 84.2 | 83.5 | 71.7 |
| **Ce** | 40.8 | 0.65 | 39 | 39.9 | 0.41 | 38 | 38.6 | 1.41 | 38.4 | 216 | 211 | 180 |
| **Pr** | 5.88 | 0.13 | 5.7 | 5.86 | 0.11 | | 37.3 | 1.32 | 37.2 | 31.1 | | 25.7 |
| **Nd** | 25 | 0.99 | 25.2 | 24.5 | 0.43 | 25 | 35.3 | 1.29 | 35.2 | 127 | | 102 |
| **Sm** | 6.68 | 0.28 | 6.2 | 6.64 | 0.22 | 6.2 | 36.9 | 1.61 | 36.7 | 39 | 37.5 | 31.7 |
| **Eu** | 2.17 | 0.09 | 2.06 | 2.14 | 0.09 | | 34.6 | 1.43 | 34.4 | 2.82 | 2.72 | 2.47 |
| **Gd** | 6.73 | 0.26 | 6.4 | 6.74 | 0.33 | 6.3 | 37.2 | 1.67 | 37 | 45.5 | 45.4 | 35.7 |
| **Tb** | 0.96 | 0.06 | 0.96 | 0.98 | 0.05 | 0.9 | 36.2 | 1.66 | 35.9 | 7.65 | 7.9 | 6.31 |
| **Dy** | 5.43 | 0.28 | 5.2 | 5.55 | 0.34 | | 36.2 | 1.61 | 36 | 47.8 | | 40.9 |
| **Ho** | 0.98 | 0.06 | 0.99 | 1.01 | 0.06 | 1.04 | 38.1 | 1.67 | 37.9 | 10.1 | | 8.39 |
| **Er** | 2.57 | 0.18 | 2.4 | 2.65 | 0.21 | | 37.7 | 1.8 | 37.4 | 28.7 | | 24.3 |
| **Tm** | 0.34 | 0.02 | 0.33 | 0.36 | 0.02 | | 37.8 | 1.71 | 37.6 | 4.16 | | 3.58 |
| **Yb** | 2 | 0.12 | 2.02 | 2.03 | 0.1 | 2 | 40.2 | 1.83 | 40 | 25.6 | 24.4 | 22.4 |
| **Lu** | 0.28 | 0.02 | 0.29 | 0.29 | 0.03 | 0.28 | 38 | 1.58 | 37.7 | 3.42 | 3.4 | 3.14 |
| **Hf** | 4.45 | 0.5 | 4.38 | 4.59 | 0.44 | 4.1 | 35.2 | 1.45 | 34.8 | 28.6 | 31.6 | 22.8 |
| **Ta** | 1.15 | 0.1 | 1.23 | 1.22 | 0.11 | 1.4 | 40.2 | 1.85 | 39.8 | 3.46 | 4.6 | 3.01 |
| **Pb** | 2.13 | 0.29 | 2.6 | 3.19 | 0.19 | | 39.1 | 2.83 | 39 | 9.39 | | 7.67 |
| **Th** | 1.19 | 0.08 | 1.08 | 1.27 | 0.11 | 1.2 | 37.6 | 1.86 | 37.2 | 14.7 | 10 | 13.7 |
| **U** | 0.41 | 0.03 | 0.42 | 0.41 | 0.02 | | 37.5 | 1.51 | 37.2 | 3.96 | 2.8 | 3.32 |

**Table 1 (continued)** Trace element data for samples analyzed in this study by ICP-MS

| | 14310,661[S] Impact melt | Lit. values[5,6,7,8,] | 14321,1180[L] Ol. Vit. | Lit. Values[9] | 14321,1539[S] Ol. Vit. | Lit. values[10] | 14321,1162[L] TFB | Lit. values[11] | 14072,44[S] High-Al | Lit. values[5,7] |
|---|---|---|---|---|---|---|---|---|---|---|
| **Be** | 5.28 | 4.2 | 45.6 | | 5.14 | | 32.4 | | 0.8 | |
| **Sc** | 21.9 | 25 | | 17.62 | 20.8 | 17.7 | | 75.8 | 51.6 | 47.1 |
| **V** | 35.7 | 38 | 47.4 | | 46.3 | 41 | 70.4 | 98 | 104 | |
| **Cr** | 1143 | 1080 | 1791 | 1605 | 1335 | 1450 | 1946 | 2550 | 2994 | 2500 |
| **Co** | 29.9 | 17 | 30.6 | 38.2 | 47.4 | 40.7 | 15.1 | 24.6 | 39.7 | 32 |
| **Ni** | 142 | 120 | 149 | 340 | 388 | 380 | 332 | 10 | 52.4 | 31 |
| **Cu** | 14.6 | 9 | 83.3 | | 10.9 | | 64.1 | | NA | |
| **Ga** | 5.6 | 3.2 | 11.2 | | 79.2 | | 4.44 | | 5.2 | 3.8 |
| **Rb** | 13.5 | 15 | 16.2 | 27 | 15.2 | | 4.64 | 21 | 1.55 | 1.3 |
| **Sr** | 194 | 175 | 133 | 176 | 140 | | 66.4 | 60 | 93.4 | 106 |
| **Y** | 182 | 185 | 187 | | 178 | | 87.4 | | 41.4 | 74 |
| **Zr** | 853 | 610 | 818 | 810 | 793 | | 285 | 500 | 141 | 172 |
| **Nb** | 60.8 | 29 | 67.4 | | 61.6 | | 24.6 | | 12.9 | 13 |
| **Mo** | 0.17 | | | | 0.21 | | | | 0.16 | |
| **Sn** | 0.03 | | | | 0.16 | | | | | 0.3 |
| **Sb** | 0.01 | 0.004 | | | 0.10 | | | | | |
| **Cs** | 0.53 | 0.7 | 0.61 | 0.66 | 0.58 | 0.66 | 0.28 | 0.3 | 0.12 | |
| **Ba** | 683 | 780 | 661 | 730 | 739 | 730 | 205 | 340 | 107 | 120 |
| **La** | 58.5 | 59 | 63.1 | 57.1 | 60.8 | 57.5 | 22.9 | 34.5 | 7.8 | 8.7 |
| **Ce** | 151.09 | 207 | 158 | 156 | 154 | 150 | 58 | 91.9 | 20.2 | 27 |
| **Pr** | 21.3 | 23 | 20.9 | | 23.3 | | 8.01 | | 2.87 | 3.2 |
| **Nd** | 87 | 91 | 93 | 92 | 90.7 | 87 | 35.8 | 56 | 12.9 | 13 |
| **Sm** | 26.8 | 23 | 24.9 | 24 | 25 | 24.5 | 10.8 | 16.9 | 4.21 | 4.4 |
| **Eu** | 2.23 | 2.28 | 2.12 | 1.96 | 1.99 | 2.02 | 0.81 | 1.05 | 0.98 | 0.97 |
| **Gd** | 30.3 | 29 | 29.5 | | 31 | | 13.0 | | 5.23 | 6.4 |
| **Tb** | 5.18 | 4.2 | 5.42 | 5.92 | 5.27 | 4.9 | 2.42 | 3.68 | 1.02 | 0.93 |
| **Dy** | 33.3 | 29 | 36.4 | | 34.7 | | 16.5 | | 6.95 | 5.9 |
| **Ho** | 6.79 | 6.8 | 7.83 | | 7.46 | | 3.85 | | 1.46 | 1.6 |
| **Er** | 19.9 | 19 | 22.1 | | 21.5 | | 10.5 | | 4.28 | 4.7 |
| **Tm** | 2.93 | 3 | 3.07 | | 3.13 | | 1.66 | | 0.64 | 0.76 |
| **Yb** | 18.7 | 16 | 20.5 | 19.5 | 19.5 | 17.3 | 11.6 | 13.4 | 4.01 | 7.7 |
| **Lu** | 2.59 | 2.76 | 2.93 | 2.62 | 2.7 | 2.3 | 1.64 | 2.02 | 0.59 | 0.61 |
| **Hf** | 19.5 | 18 | 19.6 | 21.8 | 20.3 | 21.1 | 8.04 | 12 | 3.68 | 6.9 |
| **Ta** | 2.36 | 2.3 | 2.93 | 2.53 | 2.52 | 2.29 | 1.37 | 1.79 | 0.73 | |
| **Pb** | 6.65 | 13 | 2.35 | | 8.15 | | 0.7 | | 0.43 | 1.3 |
| **Th** | 11.2 | 12 | 12.8 | 11.19 | 12 | 11.6 | 3.53 | 4.6 | 1.02 | 1.04 |
| **U** | 2.97 | 3 | 3.5 | 2.92 | 3.17 | 3.4 | 0.9 | 1.2 | 0.29 | 0.29 |

**Table 1 (continued)** Trace element data for samples analyzed in this study by ICP-MS

| | 14321,1161[L] (Group A) | Lit. values[11] | 14321,1422[L] (Group A) | Lit. values[12,13] | 14321,1582[S] (Group A) | Lit. values[14] | 14321,9075[S] (Group B) | Lit. values[4] | 14321,1179[L] (Group B) | Lit. values[11] | 14321,1183[L] (Group B) | Lit. values[11] | 14321,1184[L] (Group B) | Lit. values[11] |
|---|---|---|---|---|---|---|---|---|---|---|---|---|---|---|
| **Be** | | | | | 0.72 | | 1.41 | | | | | | | |
| **Sc** | | 61.1 | | 64.1 | | 65.7 | 60.3 | 56 | | 57.9 | | 59.4 | | 58.1 |
| **V** | 99.4 | 106 | 143 | | 174 | 149 | 109 | 102 | 112 | 122 | 117 | 101 | 96.7 | 90 |
| **Cr** | 2686 | 3660 | 3835 | 3770 | 3545 | 4250 | 2437 | 2463 | 3350 | 3870 | 3629 | 3170 | 3274 | 2800 |
| **Co** | | 34.1 | | 32 | 45.4 | 35.8 | 34.8 | 28 | | 36.8 | | 30.1 | | 32.1 |
| **Ni** | | 20 | | | 68.6 | <170 | 41.8 | | 104 | 120 | | 20 | | 40 |
| **Cu** | 40 | | 32.1 | | 30 | | 22.3 | | 96.5 | | 74.1 | | | |
| **Ga** | 2.01 | | 3.24 | | 6.42 | | 3.76 | | 3.73 | | 4.41 | | 4.33 | |
| **Rb** | 0.8 | 13 | 1.49 | 0.9 | 1.09 | | 2.88 | | 2.56 | 17 | 2.32 | 10 | 1.97 | 13 |
| **Sr** | 56 | 20 | 66.6 | 87 | 73.2 | | 115 | | 85 | 60 | 89.6 | 110 | 91.5 | 50 |
| **Y** | 20.1 | | 23.2 | | 29.2 | | 89.9 | | 64.5 | | 62.5 | | 78.1 | |
| **Zr** | 46.8 | | 55.4 | | 67 | | 380 | 220 | 266 | 350 | 251 | | 318 | |
| **Nb** | 5.14 | | 6.09 | | 6.84 | | 22.9 | | 16 | | 16.5 | | 19.6 | |
| **Mo** | | | | | 0.14 | | 0.17 | | | | | | | |
| **Sn** | | | | | *0.26* | | *0.37* | | | | | | | |
| **Sb** | | | | | *0.15* | | 0.27 | | | | | | | |
| **Cs** | 0.09 | 0.05 | 0.16 | | 0.14 | 0.56 | 0.16 | | 0.24 | 0.17 | 0.24 | 0.15 | 0.37 | 0.28 |
| **Ba** | 30.6 | 32 | 37.5 | 28 | 39.5 | | 193 | 160 | 139 | 180 | 134 | 170 | 167 | 170 |
| **La** | 2.62 | 2.89 | 3.28 | 3.19 | 3.52 | 3.11 | 25.0 | 25.2 | 19.4 | 20.1 | 17 | 18.93 | 22.9 | 24.2 |
| **Ce** | 7.12 | 8.4 | 8.79 | 9.3 | 9.61 | 7 | 69.0 | 50 | 52.0 | 57.4 | 45 | 50.5 | 59.5 | 66.1 |
| **Pr** | 1.08 | | 1.19 | | 1.53 | | 10.2 | | 7.34 | | 6.54 | | 8.39 | |
| **Nd** | 5.46 | 5.7 | 6.25 | 4.3 | 6.42 | 5.1 | 43.5 | | 34.6 | 37 | 31.1 | 31.5 | 38.6 | 43 |
| **Sm** | 1.74 | 2.11 | 2.09 | 2.10 | 2.22 | 2.15 | 13.5 | 12.7 | 9.81 | 10.7 | 8.97 | 9.57 | 11.5 | 12.6 |
| **Eu** | 0.52 | 0.56 | 0.58 | 0.62 | 0.67 | 0.73 | 1.47 | 1.38 | 1.05 | 1.2 | 1.11 | 1.21 | 1.24 | 1.4 |
| **Gd** | 2.48 | | 2.98 | | 3.04 | | 15.6 | | 10.8 | | 10.5 | | 12.9 | |
| **Tb** | 0.46 | 0.57 | 0.58 | 0.68 | 0.6 | 0.69 | 2.64 | 2.49 | 1.88 | 2.34 | 1.81 | 2.21 | 2.3 | 2.15 |
| **Dy** | 3.25 | | 3.88 | 4.39 | 4.25 | | 16.6 | | 12.6 | | 11.8 | | 15 | |
| **Ho** | 0.83 | | 0.91 | | 0.99 | | 3.47 | | 2.7 | | 2.60 | | 3.15 | |
| **Er** | 2.5 | | 2.85 | | 3.02 | | 9.60 | | 7.23 | | 7.4 | | 8.66 | |
| **Tm** | 0.38 | | 0.44 | | 0.5 | | 1.35 | | 1 | | 1.08 | | 1.23 | |
| **Yb** | 2.66 | 2.89 | 3.04 | 3.02 | 2.93 | 2.9 | 8.26 | 8.2 | 6.26 | 6.82 | 6.50 | 6.8 | 7.77 | 7.98 |
| **Lu** | 0.39 | 0.47 | 0.46 | 0.44 | 0.47 | 0.41 | 1.17 | 1.23 | 0.89 | 1.05 | 0.90 | 0.95 | 1.14 | 1.22 |
| **Hf** | 1.33 | 1.78 | 1.66 | 1.7 | 1.96 | 2 | 8.89 | 8.2 | 6.92 | 8.3 | 6.47 | 7.57 | 8.57 | 9.55 |
| **Ta** | 0.32 | 0.46 | 0.39 | 0.45 | 0.43 | 0.46 | 1.21 | 1.2 | 0.89 | 0.94 | 0.95 | 0.94 | 1.15 | 1.1 |
| **Pb** | 0.32 | | 0.82 | | 1.19 | | 1.22 | | 0.45 | | 0.51 | | 0.79 | |
| **Th** | 0.39 | 0.2 | 0.53 | 0.2 | 0.51 | 0.4 | 2.56 | 2.2 | 1.97 | 2.53 | 1.79 | 1.55 | 2.23 | 2.3 |
| **U** | 0.11 | 0.14 | 0.15 | 0.2 | 0.14 | 2.2 | 0.65 | | 0.53 | 0.62 | 0.49 | 0.52 | 0.60 | 0.3 |

**Table 1 (continued)** Trace element data for samples analyzed in this study by ICP-MS

| | 14321,1185[L] (Group B) | Lit. values[11] | 14321,1210[L] (Group B) | Lit. values[11] | 14321,1318[L] (Group B) | Lit. values[12] | 14321,1338[L] (Group B) | Lit. values[12] | 14321,1345[L] (Group B) | Lit. values[12] | 14321,1347[L] (Group B) | Lit. values[12] | 14321,1365[L] (Group B) | Lit. values[12] |
|---|---|---|---|---|---|---|---|---|---|---|---|---|---|---|
| **Be** | | | | | | | | | | | | | | |
| **Sc** | | 60.3 | | 57.8 | | 59.7 | | 58.2 | | 61.6 | | 60.4 | | 59.4 |
| **V** | 106 | 122 | 103 | 114 | 124 | | 114 | | 130 | | 102 | | 129 | |
| **Cr** | 3116 | 3370 | 2296 | 2780 | 4313 | 3819 | 3398 | 3188 | 4000 | 3264 | 2965 | 2870 | 3465 | 3470 |
| **Co** | | 29.8 | | 27.2 | 30.7 | 33.4 | | 34 | 35.4 | 33.9 | 39.6 | 31.8 | | 34.7 |
| **Ni** | | 20 | | 40 | | 100 | 50.5 | 115 | | 120 | | 72 | 129 | 125 |
| **Cu** | | | | | | | | | | | | | 23.5 | |
| **Ga** | 4.71 | | 4.14 | | 7.31 | | 11.8 | | 9.7 | | 10.2 | | 5.43 | |
| **Rb** | 2.81 | 14 | 2.94 | 13 | 3.64 | 9 | 6.74 | 13 | 4.94 | 9 | 4.74 | 9 | 3.89 | 10 |
| **Sr** | 85.6 | 10 | 91.1 | 50 | 96.9 | 72 | 97.4 | 160 | 109 | 100 | 101 | 85 | 92.1 | 100 |
| **Y** | 66.3 | | 68.3 | | 77.7 | | 76.2 | | 88 | | 86 | | 68.3 | |
| **Zr** | 256 | 350 | 271 | | 301 | 280 | 321 | 285 | 334 | 380 | 364 | 400 | 297 | 300 |
| **Nb** | 16.9 | | 17.6 | | 19.3 | | 19.9 | | 24.4 | | 20.1 | | 18.2 | |
| **Mo** | NA | | NA | | NA | | NA | | NA | | NA | | NA | |
| **Sn** | | | | | | | | | | | | | | |
| **Sb** | | | | | | | | | | | | | | |
| **Cs** | 0.31 | 0.11 | 0.26 | 0.36 | 0.70 | 0.18 | 0.61 | 0.3 | *1.18* | 0.29 | *1.08* | 0.26 | 0.25 | 0.24 |
| **Ba** | 141 | 140 | 151 | 175 | 157 | 160 | 183 | 200 | 212 | 200 | 199 | 190 | 160 | 170 |
| **La** | 18.2 | 19.5 | 20.2 | 19.7 | 22.4 | 20.8 | 21.8 | 22.8 | 23.4 | 22.7 | 24.1 | 24.9 | 21.9 | 20.5 |
| **Ce** | 47.3 | 53.4 | 54 | 53.8 | 58.8 | 59.7 | 57.9 | 63.8 | 64.3 | 63.2 | 64.3 | 67.9 | 53.2 | 57.1 |
| **Pr** | 6.86 | | 7.81 | | 8.86 | | 8.41 | | 8.65 | | 9.95 | | 7.24 | |
| **Nd** | 32.7 | 36 | 34.6 | 36 | 38.5 | 30 | 37.6 | 40 | 44.0 | 42 | 42.9 | 40 | 35.6 | 33 |
| **Sm** | 9.49 | 10.4 | 9.79 | 10.2 | 11.3 | 10.4 | 11.3 | 10.8 | 11.3 | 11.6 | 13.1 | 11.9 | 11.3 | 10.5 |
| **Eu** | 1.03 | 1.24 | 1.33 | 1.2 | 1.27 | 1.27 | 1.25 | 1.33 | 1.6 | 1.37 | 1.33 | 1.43 | 1.4 | 1.26 |
| **Gd** | 10.1 | | 10.8 | | 13.0 | | 12.6 | | 13.5 | | 15.3 | | 11.6 | |
| **Tb** | 1.79 | 2.27 | 1.97 | 2.36 | 2.28 | 2.4 | 2.29 | 2.52 | 2.45 | 2.67 | 2.61 | 2.71 | 2.04 | 2.32 |
| **Dy** | 12.1 | | 13.0 | | 15.1 | | 15.1 | | 17.0 | | 16.3 | | 13.0 | |
| **Ho** | 2.65 | | 2.77 | | 2.87 | | 3.1 | | 3.72 | | 3.47 | | 2.95 | |
| **Er** | 7.09 | | 7.68 | | 8.24 | | 8.55 | | 10.4 | | 9.76 | | 8.19 | |
| **Tm** | 1.04 | | 1.08 | | 1.17 | | 1.19 | | 1.41 | | 1.43 | | 1.22 | |
| **Yb** | 6.67 | 6.92 | 6.94 | 6.81 | 7.48 | 7.27 | 7.86 | 7.4 | 8.72 | 7.61 | 8.57 | 8.01 | 7.67 | 7.27 |
| **Lu** | 0.92 | 1.06 | 0.97 | 1.03 | 1.03 | 0.98 | 1.07 | 1 | 1.26 | 1.09 | 1.12 | 1.09 | 1.04 | 0.97 |
| **Hf** | 6.47 | 8.9 | 7.24 | 8.13 | 8.09 | 8.15 | 8.39 | 8.43 | 8.61 | 8.58 | 9.10 | 9 | 8.28 | 7.95 |
| **Ta** | 0.92 | 0.97 | 0.98 | 0.93 | 1.13 | 1.08 | 1.11 | 1.11 | 1.25 | 1.05 | 1.28 | 1.2 | 1.16 | 0.99 |
| **Pb** | 0.71 | | 0.42 | | 0.90 | | 1.61 | | 0.76 | | 1.02 | | 0.79 | |
| **Th** | 1.92 | 1.75 | 2 | 1.52 | 2.37 | 1.73 | 2.56 | 1.98 | 3.04 | 1.95 | 2.70 | 2.33 | 2.38 | 1.79 |
| **U** | 0.52 | 0.53 | 0.53 | 0.3 | 0.63 | 0.44 | 0.67 | 0.7 | 0.81 | 0.57 | 0.69 | 0.58 | 0.66 | 0.42 |

**Table 1 (continued)** Trace element data for samples analyzed in this study by ICP-MS

| | 14321,1425[L] (Group B) | Lit. values[12] | 14321,1429[L] (Group B) | Lit. values[13] | 14321,1448[S] (Group B) | Lit. values[14] | 14321,1449[S] (Group B) | Lit. values[14] | 14321,1535[S] (Group B) | Lit. values[14] | 14321,1585[S] (Group B) | Lit. values[14] | 14321,9048[S] (Group B) | Lit. values[4] |
|---|---|---|---|---|---|---|---|---|---|---|---|---|---|---|
| **Be** | | | | | 1.29 | | 1.12 | | 1.06 | | 1.25 | | 1.39 | |
| **Sc** | | 58.1 | | 61.3 | 65.1 | 59 | 68.4 | 61.5 | 68.8 | 58.2 | 58.2 | 59.2 | 65.1 | 60 |
| **V** | 102 | | 119 | | 148 | 118 | 147 | 119 | 125 | 112 | 112 | 115 | 109 | 100 |
| **Cr** | 2470 | 3073 | 2533 | 2975 | 4027 | 3840 | 2843 | 2690 | 2308 | 3330 | 2588 | 2790 | 2566 | 2532 |
| **Co** | | 29.9 | | 37.4 | 41.5 | 34.9 | 33.4 | 26.2 | 39.1 | 30.2 | 38.4 | 30.4 | 35.7 | 27 |
| **Ni** | | 80 | | 70 | 37.1 | 61 | 21 | <140 | 42 | 48 | 31 | | 30.2 | |
| **Cu** | 24.5 | | 57.2 | | 17.2 | | 23.8 | | 21.1 | | 22.5 | | 25.7 | |
| **Ga** | 5.32 | | 6.02 | | 3.94 | | 0.33 | | 10.5 | | 2.8 | | 3.68 | |
| **Rb** | 2.61 | 10 | 2.59 | 10 | 2.71 | | 2.83 | | 2.38 | | 2.57 | | 2.96 | |
| **Sr** | 86.1 | 70 | 100 | 84 | 103 | | 125 | | 115 | | 105 | | 116 | |
| **Y** | 72.1 | | 84.0 | | 70.2 | | 97.5 | | 77.2 | | 85.2 | | 90.7 | |
| **Zr** | 300 | 370 | 333 | 400 | 292 | | 369 | | 318 | | 342 | | 382 | |
| **Nb** | 19.6 | | 21.3 | | 17.9 | | 21.6 | | 18.9 | | 20.0 | | 22.8 | |
| **Mo** | NA | | NA | | 0.19 | | 0.17 | | 0.21 | | 0.18 | | 0.18 | |
| **Sn** | | | | | 0.07 | | 0.09 | | 0.23 | | 0.04 | | 0.05 | |
| **Sb** | | | | | 0.11 | | 0.06 | | 0.14 | | 0.05 | | 0.05 | |
| **Cs** | 0.26 | 0.11 | 0.28 | 0.13 | 0.12 | <1.2 | 0.12 | <1 | 0.08 | 0.6 | 0.10 | | 0.11 | |
| **Ba** | 163 | 190 | 186 | 190 | 171 | 210 | 195 | 190 | 173 | 160 | 174 | 180 | 191 | 150 |
| **La** | 21.4 | 23.7 | 23.6 | 23.3 | 23 | 20.4 | 26.5 | 24.5 | 23.1 | 20.3 | 22.6 | 22.3 | 25.2 | 25 |
| **Ce** | 56.2 | 60.9 | 63.6 | 62.3 | 57.9 | 52 | 69 | 65 | 61.3 | 53 | 63.5 | 58.9 | 69.4 | 66 |
| **Pr** | 7.67 | | 9.03 | | 8.74 | | 10.2 | | 9.15 | | 9.15 | | 10.2 | |
| **Nd** | 35.9 | 39 | 40.3 | 41 | 37.7 | 37 | 41.8 | 42 | 37.3 | 32 | 39.6 | | 43.2 | |
| **Sm** | 10.7 | 12 | 12 | 12.1 | 10.8 | 10.5 | 12.4 | 12.1 | 10.9 | 9.93 | 12.2 | 11.1 | 13.6 | 12 |
| **Eu** | 1.01 | 1.37 | 1.37 | 1.35 | 1.28 | 1.31 | 1.45 | 1.52 | 1.38 | 1.33 | 1.36 | 1.43 | 1.41 | 1.48 |
| **Gd** | 12.9 | | 13.2 | | 13.6 | | 15.5 | | 13.4 | | 13.9 | | 15.5 | |
| **Tb** | 2.30 | 2.63 | 2.25 | 2.52 | 2.30 | 2.1 | 2.65 | 2.6 | 2.43 | 2 | 2.47 | 2.1 | 2.69 | 2.56 |
| **Dy** | 13.6 | | 15.8 | | 15.1 | | 16.9 | | 15.5 | | 15.3 | | 16.7 | |
| **Ho** | 2.99 | | 3.49 | | 3.12 | | 3.52 | | 3.22 | | 3.23 | | 3.37 | |
| **Er** | 8.11 | | 9.13 | | 8.95 | | 9.95 | | 9.12 | | 8.89 | | 9.53 | |
| **Tm** | 1.13 | | 1.32 | | 1.28 | | 1.44 | | 1.32 | | 1.3 | | 1.35 | |
| **Yb** | 7.52 | 7.88 | 8.32 | 7.93 | 7.76 | 6.6 | 8.84 | 7.9 | 7.82 | 6.5 | 7.79 | 7 | 8.40 | 8.3 |
| **Lu** | 1.14 | 1.09 | 1.18 | 1.11 | 1.11 | 0.92 | 1.28 | 0.99 | 1.12 | 0.87 | 1.09 | 0.94 | 1.18 | 1.31 |
| **Hf** | 7.74 | 8.64 | 8.57 | 8.62 | 7.85 | 8.3 | 9.49 | 9.8 | 8.24 | 8.1 | 8.70 | 8.7 | 9.08 | 9.1 |
| **Ta** | 1.1 | 1.15 | 1.22 | 1.15 | 1.03 | 0.92 | 1.23 | 1.05 | 1.04 | 0.98 | 1.08 | 0.98 | 1.30 | 1.3 |
| **Pb** | 0.85 | | 0.97 | | 2.54 | | 1.67 | | 1.15 | | 1.71 | | 1.17 | |
| **Th** | 2.36 | 2.04 | 2.56 | 2.4 | 2.25 | 1.9 | 2.60 | 2.3 | 2.28 | 1.9 | 2.27 | 2.1 | 2.61 | 2.5 |
| **U** | 0.64 | 0.62 | 0.66 | 0.58 | 0.58 | 1.1 | 0.68 | 1 | 0.63 | 1.2 | 0.59 | 1.3 | 0.66 | |

**Table 1 (continued)** Trace element data for samples analyzed in this study by ICP-MS

| | 14053,240[S] (Group C) | Lit. values[4,15,16] | 14321,1344[L] (Group C) | Lit. values[12] | 14321,1432[L] (Group C) | Lit. values[12] | 14321,1524[S] (Group C) | Lit. values[12] | 14321,1568[S] (Group C) | Lit. values[12] | 14321,1573[S] (Group C) | Lit. values[14] | 14321,1578[S] (Group C) | Lit. values[14] |
|---|---|---|---|---|---|---|---|---|---|---|---|---|---|---|
| **Be** | 1.61 | | | | | | 0.76 | | 0.72 | | 0.88 | | 0.48 | |
| **Sc** | 57.6 | 55 | | 59.7 | | 62 | 62.9 | 60.8 | 64.5 | 55.4 | 61.8 | 59.5 | 60.3 | 52.9 |
| **V** | 110 | | 103 | | 124 | | 146 | 129 | 122 | 119 | 138 | 134 | 132 | 131 |
| **Cr** | 2120 | 2860 | 3597 | 3386 | 2729 | 2920 | 2984 | 4230 | 2977 | 3280 | 3731 | 4040 | 3821 | 3720 |
| **Co** | 30.7 | 25 | 34.9 | 34.6 | *21* | 28 | 48.7 | 39.5 | 41.1 | 31.7 | 42.9 | 35.4 | 48.7 | 38.4 |
| **Ni** | 20.5 | 14 | | 150 | | | 86.1 | 105 | 61.6 | 50 | 61.3 | 70 | 80 | 73 |
| **Cu** | 31.8 | | | | | | 35.1 | | 21.7 | | 23.7 | | 21.8 | |
| **Ga** | 2.81 | 4.8 | 9.07 | | 5.15 | | 3.97 | | 3.27 | | 3.86 | | 2.89 | |
| **Rb** | 2.58 | 2.1 | 5.04 | 13 | 1.55 | <8 | 1.83 | | 1.34 | | 1.65 | | 0.99 | |
| **Sr** | 105 | 98.6 | 90.3 | 150 | 83.2 | 60 | 102 | | 69.7 | | 88.2 | | 56.5 | |
| **Y** | 64.5 | 54.7 | 64.5 | | 50.9 | | 57.9 | | 39.9 | | 56 | | 28.3 | |
| **Zr** | 257 | 215 | 226 | 390 | 191.4 | 300 | 208 | | 141 | | 202 | | 92.3 | |
| **Nb** | 19.2 | 15.7 | 18.5 | | 14.5 | | 15.4 | | 10.8 | | 16.3 | | 7.45 | |
| **Mo** | 0.15 | | | | | | 0.20 | | 0.17 | | 0.14 | | 0.16 | |
| **Sn** | 0.08 | | | | | | 0.06 | | 0.03 | | 0.04 | | 0.02 | |
| **Sb** | bdl | | | | | | 0.11 | | 0.03 | | 0 | | 0.01 | |
| **Cs** | 0.15 | | 0.88 | 0.26 | 0.51 | 0.15 | 0.11 | 0.5 | 0.08 | | 0.08 | | 0.05 | |
| **Ba** | 176 | 163 | 165 | 180 | 117 | 110 | 125 | | 78.7 | | 121 | | 58.4 | 80 |
| **La** | 14.1 | 12.8 | 15.2 | 21 | 12.0 | 11.9 | 12.8 | 11.7 | 7.75 | 7.19 | 11.5 | 11.7 | 5.47 | 5.13 |
| **Ce** | 37.2 | 36.4 | 39.7 | 58.4 | 30.5 | 31.2 | 32.0 | 28.4 | 21.9 | 19 | 32.1 | 30 | 15.1 | 13.4 |
| **Pr** | 5.25 | | 5.98 | | 4.21 | | 4.55 | | 3.18 | | 4.64 | | 2.2 | |
| **Nd** | 23.6 | 22 | 26.4 | 35 | 20.5 | 18 | 21.1 | 18 | 15.2 | | 22.1 | | 11 | |
| **Sm** | 7.32 | 6.5 | 7.59 | 10.7 | 6.21 | 6.44 | 6.43 | 6.08 | 4.65 | 3.88 | 6.74 | 6.03 | 3.31 | 2.85 |
| **Eu** | 1.20 | 1.23 | 1.04 | 1.24 | 0.93 | 1.03 | 1.01 | 1.11 | 0.70 | 0.71 | 0.98 | 1.06 | 0.52 | 0.59 |
| **Gd** | 8.35 | 8.5 | 8.25 | | 7.9 | | 8.23 | | 5.61 | | 8.14 | | 4.01 | |
| **Tb** | 1.48 | 1.62 | 1.51 | 2.49 | 1.48 | 1.48 | 1.59 | 1.3 | 1.05 | 0.7 | 1.48 | 1.6 | 0.77 | 0.79 |
| **Dy** | 9.86 | 11.1 | 9.84 | | 9.9 | | 10.4 | | 6.92 | | 9.91 | | 5.16 | |
| **Ho** | 2.24 | 2.1 | 2.28 | | 2.14 | | 2.33 | | 1.49 | | 2.10 | | 1.09 | |
| **Er** | 6.36 | 6.51 | 6.48 | | 6.15 | | 6.86 | | 4.36 | | 6.24 | | 3.29 | |
| **Tm** | 0.92 | | 0.95 | | 0.88 | | 0.93 | | 0.65 | | 0.92 | | 0.5 | |
| **Yb** | 6.21 | 6.1 | 6.48 | 6.97 | 6.11 | 5.7 | 6.22 | 5.3 | 4.28 | 3.6 | 6.15 | 5.6 | 3.44 | 2.9 |
| **Lu** | 0.95 | 0.89 | 0.86 | 1.07 | 0.91 | 0.82 | 0.97 | 0.75 | 0.63 | 0.56 | 0.86 | 0.79 | 0.48 | 0.46 |
| **Hf** | 6.53 | 9.8 | 5.99 | 8.06 | 5.10 | 5.02 | 6.01 | 5.4 | 3.51 | 3.4 | 4.99 | 5.2 | 2.53 | 2.3 |
| **Ta** | 1.08 | 1.2 | 1.10 | 1.03 | 0.88 | 0.89 | 1.05 | 0.74 | 0.57 | 0.5 | 0.82 | 0.77 | 0.42 | 0.38 |
| **Pb** | 1.14 | | 0.92 | | 1.09 | | 1.38 | | 0.73 | | 0.92 | | 0.68 | |
| **Th** | 1.98 | | 1.96 | 2.1 | 1.73 | 1.46 | 1.82 | 1.5 | 1.12 | 0.9 | 1.69 | 1.5 | 0.88 | 0.7 |
| **U** | 0.51 | | 0.52 | 0.39 | 0.51 | 0.32 | 0.49 | | 0.31 | | 0.45 | | 0.22 | |

*Notes:* 1 = Chazey et al. (2003); 2 = Wilson (1998); 3 = Pearce et al. (1996) 4 = Dickinson et al. (1985); 5 = Taylor et al. (1972); 6 = Rose et al. (1972); 7 = Helmke et al. (1972); 8 = Brunfelt et al. (1972); 9 = Shervais et al. (1988); 10 = Neal and Taylor (1989); 11 = Shervais et al. (1985); 12 = Neal et al. (1988); 13 = Hughes et al. (1990); 14 = Neal et al. (1989b); 15 = Hubbard et al. (1972); 16 = Willis et al. (1972). S = Solution ICP-MS analysis; L = LA-ICP-MS analysis. Lit. value = Literature value; Ref. value = Reference value. TFB = Tridymite FerroBasalt. See text for discussion of errors. NA = Not Analyzed; bdl = below detection limit.

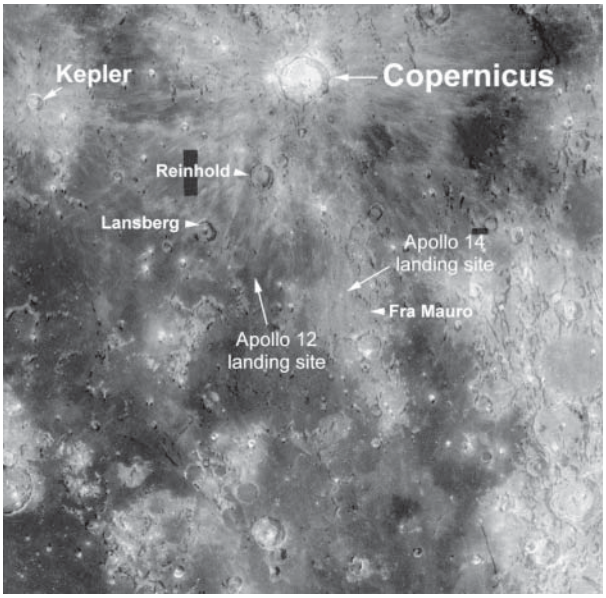


**FIGURE 1.** Map of Fra Mauro region depicting major impact craters. Northernmost portion of map lies just south of rim of Mare Imbrium. Produced from the Clementine 750 nm data set.

ITE-rich groups (1 through 4) could be generated by a parental magma similar in composition to that of their most ITE-depleted basalts (Group 5) assimilating varying amounts of a KREEP component. Shervais et al. (1985) also invoked KREEP assimilation to generate their most ITE-rich basalts, but suggested different degrees of partial melting of at least two sources could not be ruled out for the other basaltic compositions. Both studies treated assimilation as a bulk mixing process between an ITE-depleted parent magma and a KREEP component.

Neal et al. (1988, 1989a, 1989b) concluded that as more data became available, the Apollo 14 high-Al basalts would prove to form a continuum of compositions rather than discrete groups (Fig. 2b). These authors modeled this continuum using a single parental magma (the sample with the lowest ITE abundances—14321,1422) that experienced combined assimilation of KREEP (composition similar to Apollo 15 KREEP basalt 15386; Vaniman and Papike 1980) and fractional crystallization (AFC; DePaolo 1981). However, Shih and Nyquist (1989a, 1989b) concluded that the variability of ***Mg*** [molar Mg/(Mg+Fe)] with trace-element contents, coupled with the varying ages of the basalts, negated a single parental magma for these basalts (Fig. 3). Dasch et al. (1987) reported that virtually all the basalts lie on a single radiogenic growth curve from a primitive lunar initial at 4.56 Ga and with the source having Rb/Sr = 0.021. This relationship suggested that the Apollo 14 high-Al basalts were related by a single source that melted and erupted onto the surface at different times. Neal and Taylor (1990) incorporated this information into a revised AFC model and suggested the basalts were the products of three distinct magmatic events (at 4.3, 4.1, and 3.9 Ga) with each event following essentially the same petrogenetic pathway, namely different degrees of KREEP contamination through AFC of an ITE-depleted parental magma.

Dasch et al. (1987) also reported Sm-Nd isochrons for the

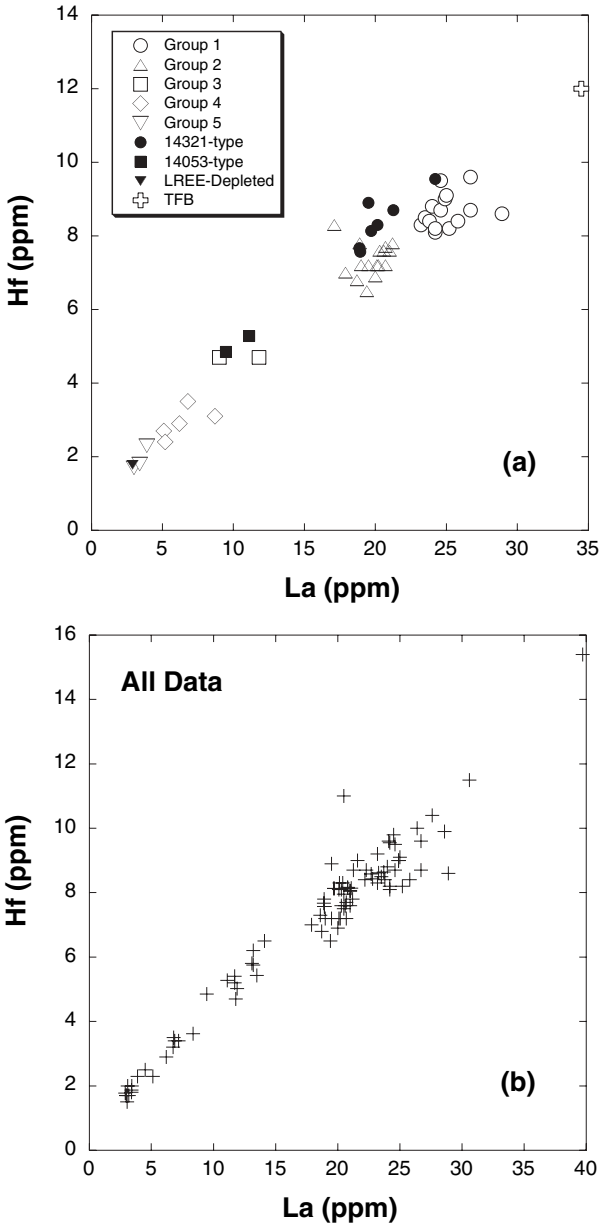


**FIGURE 2.** Relationship between La and Hf in Apollo 14 high-Al basalts. (**a**) Data from Dickinson et al. (1985) that define basalt Groups 1–5, and from Shervais et al. (1985) for the 14321-type, 14053-type, LREE-depleted, and the TFB (Tridymite FerroBasalt); (**b**) all data are plotted (Shervais et al. 1985; Dickinson et al. 1985; Neal et al. 1988, 1989b; this study). See text for discussion.

Apollo 14 high-Al basalts and noted that the ages thus derived were younger than those derived using Rb-Sr data. However, the errors associated with the Sm-Nd ages were large such that they are essentially indistinguishable from the Rb-Sr ages. Dasch et al. (1987) concluded this was a function of the small range in Sm/Nd ratios exhibited by the different mineral fractions used to construct the isochrons, which was magnified by the relatively poor precision on each Sm-Nd determination. Snyder et al. (2000) and Snyder and Taylor (2000, 2001) suggested that the

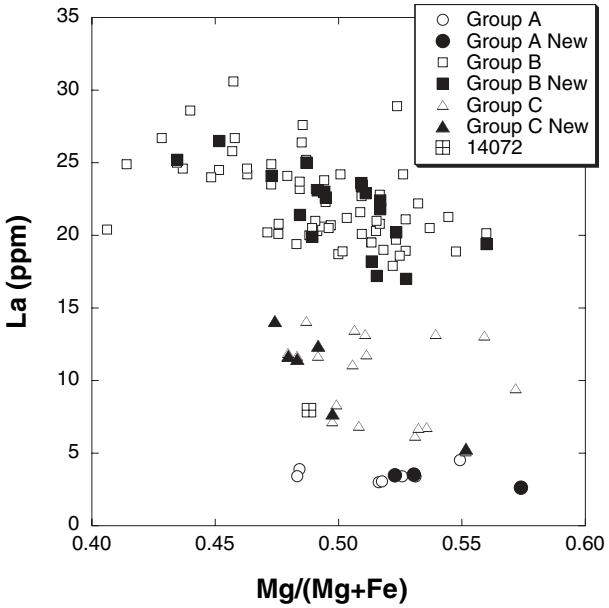


**FIGURE 3.** Relationship between **Mg** [molar Mg/(Mg + Fe)] and La (after Shih and Nyquist 1989a, 1989b) with the basalts depicted using the new classification proposed here. Data sources are as in Figure 2 along with Hubbard et al. (1972).

apparent age differences reflected a weighted average of target lithologies, such that the Apollo 14 high-Al basalts are, in fact, impact melts. They proposed that the discrepancy between Rb-Sr and Sm-Nd ages was produced by complete reequilibration of the Sm-Nd system as the impact melt cooled, but only partial reequilibration of the Rb-Sr system.

In this paper, we report new analyses of high-Al basalts that were analyzed originally by instrumental neutron activation (INA). We have analyzed these using inductively coupled plasma mass spectrometry (ICP-MS), which quantifies the petrogenetically significant elements Zr, Y, and Nb. The majority of basalt samples are clasts that have been extracted from Apollo 14 breccia 14321 (e.g., Grieve et al. 1975; Duncan et al. 1975). These data are used in a re-investigation of Apollo 14 high-Al basalt petrogenesis and, as depicted in Figure 3, these basalts could be subdivided into 3 groups, which correlate with current age data (e.g., Papanastassiou and Wasserburg 1971; Compston et al. 1971, 1972; Dasch et al. 1987; see below). The new data reported here clearly confirm the presence of at least three distinct groups of Apollo 14 high-Al basalts that were derived from distinct source regions at different times.

## METHODS

The reader is referred to Dickinson et al. (1985), Shervais et al. (1985), and Neal et al. (1988, 1989b) for petrographic descriptions of the Apollo 14 high-Al basalts, to Shervais et al. (1988) and Neal and Taylor (1989) for the petrography of the olivine vitrophyres, to Ryder (1985 and references therein) for the petrography of KREEP basalt 15386, to Warner et al. (1980) for the petrography of breccia 14168, and to Longhi et al. (1972) for the petrography of 14310 and 14072. For this study, eleven Apollo 14 high-Al basalts, the basaltic impact melt 14310 (Green et al. 1972; Walker et al. 1972; Ringwood et al. 1972; Morgan et al. 1972), Apollo 14 KREEP breccia matrix from 14168,34, and KREEP basalt 15386,48 (see also Neal and Kramer 2003) were analyzed by solution ICP-MS at University of Notre Dame (see www.nd.edu/~icpmslab for full details). Fourteen Apollo 14 high-Al basalt clasts from breccia 14321, which had been fused for major-element analysis by electron microprobe and were previously analyzed by Shervais et al. (1985) and Neal et al. (1988) using INA, were analyzed by laser ablation (LA) ICP-MS. Using LA-ICP-MS, the fused glass of the tridymite ferrobasalt 14321,1162 (Shervais et al. 1985), and two previously reported olivine vitrophyre clasts (Shervais et al. 1988; Neal and Taylor 1989) were also analyzed: 14321, 1180 by LA-ICP-MS and 14321,1539 by solution ICP-MS.

Sample digestion, preparation, and solution ICP-MS analytical procedures are detailed in Neal (2001). The final data are calculated following the method modified after Jenner et al. (1990) and reported in Neal (2001). Each of the 15 samples analyzed by solution were replicated five times (with each replicate being analyzed four times) to demonstrate reproducibility. The reference materials BHVO-1 and BHVO-2 were analyzed with the samples to check for accuracy (Table 1). The 18 fused glass samples analyzed using LA-ICP-MS were created by CRN at the University of Tennessee using the method of Brown (1977) and described by Neal et al. (1988). The bulk sample used for INA was crushed and fused and for all preparations; it was impossible to exclude the mesostasis phases from the sample analysis. The VG LaserProbe used at the University of Notre Dame was a quadrupled infrared (1064 nm) Nd:YAG laser with an emission radiation set at 266 nm, which produced 20 μm diameter ablation pits in the sample. The liberated particles were carried by argon to the plasma. Raw counts were converted into final concentrations using the LAMTRACE data reduction software of Dr. Simon Jackson of Macquarie University, Sydney, Australia (Jackson et al. 1997), with the CaO, determined by electron microprobe (Neal et al. 1988, 1989b), as the internal standard. The NIST glass 612 (Pearce et al. 1997) was used as the calibration standard.

## RESULTS

Table 1[1] lists the concentrations of elements in each sample as obtained at the Notre Dame ICP-MS facility. The ICP-MS data are in general agreement with previously published values obtained by INA (excluding sample 14168—see below). The errors associated with some of the lighter elements (Li, Be, Sc, V, Cr, Cu, Ni, Zr) were occasionally greater than 10%, although where applicable, their averaged values agreed closely with previously published data. Furthermore, reference material data collected during sample analysis give the accepted values for these elements. For the most part, however, errors were usually better than 10% (and mostly better than 5%) and also better than the quoted errors associated with INA analyses. Throughout most of the analyses of these samples, there was a significant molecular interference on Sc and Ni during some runs that was not noticed until the analyses were complete. Therefore, we only report ICP-MS data for these elements when we could demonstrate (through monitoring of CeO) that such interferences were minimal (i.e., oxides were <1%).

The previous INA results reported no more than 22 trace elements (cf. Dickinson et al. 1985; Shervais et al. 1985; Neal et al. 1988, 1989b). We can now confidently report up to 35 trace elements when analyzed by solution ICP-MS and up to 31 trace elements using laser-ablation ICP-MS. Most significantly, our ICP-MS data have quantified petrogenetically important elements (i.e., Zr, Y, and Nb), the abundances of which were heretofore

[1] Deposit item AM-06-029, Table 1 (trace element data for samples analyzed in this study by ICP-MS). Deposit items are available two ways: For a paper copy contact the Business Office of the Mineralogical Society of America (see inside front cover of recent issue) for price information. For an electronic copy visit the MSA web site at http://www.minsocam.org, go to the American Mineralogist Contents, find the table of contents for the specific volume/issue wanted, and then click on the deposit link there.

not known in the Apollo 14 high-Al basalts.

Elemental ratios (i.e., Zr/Y and Nb/Ce) divide the Apollo 14 high-Al basalts into three distinct groups (Fig. 4), which are designated Group A (Nb/Ce > 0.69), Group B (Nb/Ce < 0.4), and Group C (Nb/Ce between 0.45 and 0.55). Basalt 14072 has a Nb/Ce ratio of 0.64 and plots between Groups A and C basalts in Figure 4. On the basis of present data, these groups appear to have been derived at different times. Using the classifications of Dickinson et al. (1985): the oldest basalts (~4.3 Ga) comprise Groups 4 and 5 (hereafter referred to as Group A); the intermediate age basalts (~4.1 Ga) comprise Groups 1 and 2 (hereafter called Group B); and the youngest basalts (~3.9 Ga) comprise Group 3 basalts (referred to now as Group C).

The different groups of Apollo 14 high-Al basalts have distinctive chondrite-normalized trace-element profiles (Figs. 5a–5c). Group A basalts and 14072 exhibit Nb-Ta "humps" (Fig. 5a) that are absent in the profiles of Group B and Group C basalts (Figs. 5b and 5c). 14072 also exhibits a slight elevation of Zr and Hf, which is not seen in the Group A and Group B basalts, although Zr and Hf are slightly elevated in the profiles of Group C basalts (Fig. 5c). Group A basalts are depleted in the highly incompatible elements (Fig. 5a) and are depleted in most trace elements relative to Group B and Group C basalts. Group B basalts form a relatively tight cluster of subparallel profiles (Fig. 5b). Group C basalts exhibit more variation in relative abundance (Fig. 5c), which is also exhibited in elemental ratios (see below). All of the basalts exhibit negative anomalies at Sr and Eu (both indicative of plagioclase fractionation). There is also a slight negative Y anomaly in these basalts, which suggests clinopyroxene may have been retained in the source(s).

Dickinson et al. (1985) previously had analyzed a basalt clast from 14168. Warner et al. (1980) analyzed the same sample (subsample number 38). Both described the basalt as having a very high $K_2O$ content (0.57 wt%), but relatively low REE abundances (15× chondritic). The sample allocated for our analysis of 14168 (Table 1) was of the breccia matrix, as demonstrated by the companion thin section 14168,44. This sample contains much higher REE contents (~100× chondrites), and a profile resembling KREEP (Fig. 5d). The microfractured crystals and glassy texture of 14168,44, and its chemical similarity with known impact melt rocks (see below), classifies this sample as an impact melt breccia.

The composition of KREEP basalt 15386 (subsample 48) has

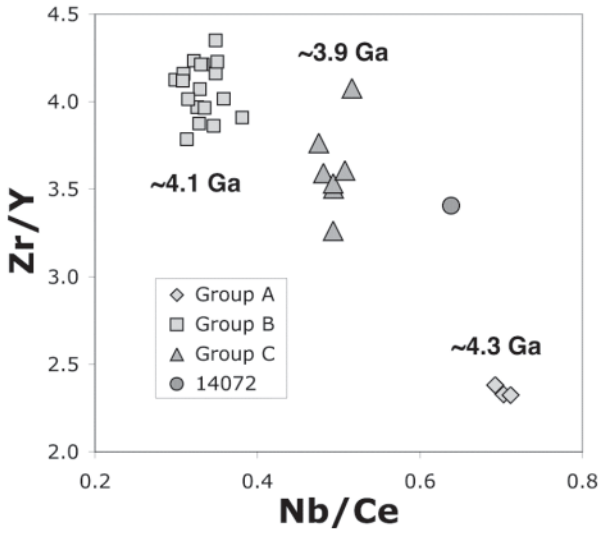


**FIGURE 4.** The new data presented in this paper for the Apollo 14 high-Al basalts subdivide these basalts into 3 groups when Nb/Ce is plotted against Zr/Y. One sample, 14072, falls between Groups A and C.

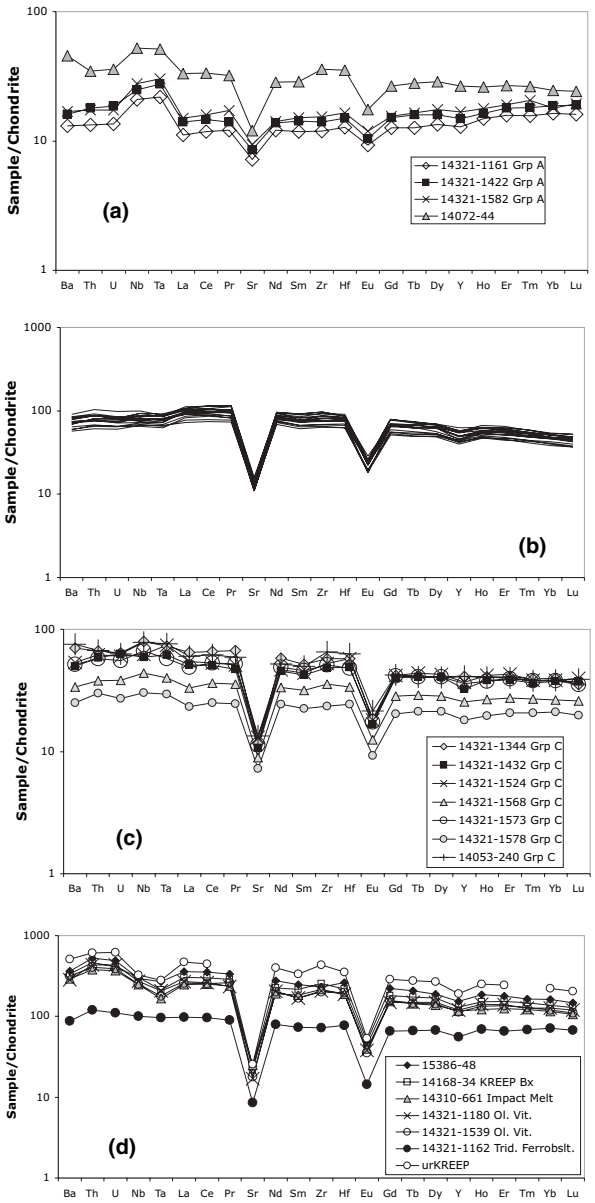


**FIGURE 5.** Chondrite-normalized trace-element profiles for (**a**) Group A high-Al basalts; (**b**) Group B high-Al basalts (a legend is not included for reasons of clarity; 18 clasts of similar composition are plotted—see Table 1 for the sample numbers); (**c**) Group C high-Al basalts; (**d**) KREEP-rich rocks from Apollo 14 and KREEP basalt 15386,48 (Bx = Breccia; Ol. Vit. = Olivine Vitrophyre; Trid. Ferrobslt. = Tridymite Ferrobasalt; urKREEP composition is from Warren and Wasson 1979). Normalizing values are from Anders and Grevesse (1989).

been reported by Neal and Kramer (2003). The new analysis is similar to the whole-rock composition reported for 15386,1 by Rhodes and Hubbard (1973), Hubbard et al. (1974), Nyquist et al. (1974), and Wiesmann and Hubbard (1975). Elemental levels are generally higher than those reported by Warren and Wasson (1978) and Warren et al. (1978) for 15386,19 and 15386,56, respectively. The chondrite-normalized incompatible element profile of impact melt 14310 is subparallel to our analysis of 15386,48 although abundances of the former are slightly lower overall (Fig. 5d).

The olivine vitrophyres (14321,1180 and -,1539) have abundances lower than KREEP basalt 15386, but exhibit normalized profiles that are parallel to that sample (Fig. 5d). The tridymite ferrobasalt 14321,1162 also exhibits a C1 normalized profile that more closely resembles the high-Al mare basalts, but is distinguished by its low ***Mg*** (0.34).

## Discussion

### Major elements

The major-element distributions of the Apollo 14 high-Al basalts reflect differences in source mineralogy and degree of partial melting among the various groups. Figures 6a–6f show the major element data for the Apollo 14 high-Al basalts as reported in the literature. The basalts have been divided into the three groups as defined in this paper. There are few coherent trends evident in these data, although some general observations can be made. For example, the Group B basalts generally have the lowest contents of MgO and Cr contents (Fig. 6c) and the highest abundances of $Al_2O_3$, CaO, $Na_2O$, and $K_2O$ (Figs. 6b, 6d, 6e, and 6f). This is broadly consistent with their having the highest ITE abundances. Similarly, Group A basalts (with the lowest ITE abundances) generally have the highest MgO and Cr (Fig. 6c), and the lowest $Al_2O_3$ and $K_2O$ contents. For example, the sample with the highest MgO content (14321,1161) contains the lowest La abundance of the Group A basalts. However, the Group C basalt with the highest MgO content (14321,1149) does not contain the lowest La abundance of basalts that form this group. Interestingly, the Group B basalts do not contain the highest $TiO_2$ contents, as would be expected if the major elements are produced by simple crystal fractionation; this distinction belongs to the Group A basalts (Fig. 6a), which on the basis of ITE abundances, are the least evolved, although a Group C basalt (14321, 1149) contains the highest $TiO_2$ content (3.94 wt%).

### Impact melts or pristine basalts?

Although basaltic impact melts have been recognized at the Apollo 14 site (e.g., 14310—Green et al. 1972; Walker et al. 1972; Ringwood et al. 1972, Morgan et al. 1972; also olivine vitrophyres—e.g., Shervais et al. 1988; Neal and Taylor 1989), these generally have unique compositions relative to the high-Al basalts (Fig. 4; Table 1). As noted above, Snyder et al. (2000) and Snyder and Taylor (2000, 2001) argued on the basis of Sr-Nd isotope systematics that the Apollo 14 high-Al basalts were impact melts. They concluded that if the $I_{Sr}$ of the basalts were recalculated assuming they actually had formed at 3.9 Ga (the time of the proposed lunar cataclysm—see Ryder 2002, and references therein), they would lie on a mixing line between Ferroan Anorthosites (FAN) and KREEP, thereby showing the high-Al basalts to be impact melts. We have attempted to reproduce this work using the Sr-isotope data of FAN 60025 (Carlson and Lugmair 1988) and KREEP basalt 15386 (Nyquist et al. 1974). In this simple mixing model (Fig. 7), KREEP is mixed with the FAN component in 5% increments, with all $^{87}Sr/^{86}Sr$ ratios calculated for an age of 3.9 Ga. As can be seen, the majority of the high-Al basalt clasts lie above this mixing line and do not form a linear array.

Ridley (1975) and Warren et al. (1997) had concluded that these basalts were pristine on the basis of low siderophile-element contents. Furthermore, Hagerty et al. (2001, 2002, 2003, 2005) analyzed individual minerals in the high-Al basalts, and showed that olivine and plagioclase in these basalts reflected the whole-rock composition, concluding that whole-rock analyses of high-Al basalts are representative, and that the spread of Apollo 14 high-Al basalt data is not the result of short-range unmixing (cf. Haskin and Korotev 1977; Lindstrom and Haskin 1978). Hagerty et al. (2001, 2002, 2003, 2005) also showed through, for example, the Ni contents of olivines that these phenocrysts are early-forming crystals in a pristine fractionating magma, with the low non-volatile/volatile ratio Ba/Rb adding further support to the contention that the high-Al basalts are pristine mare basalts.

To emphasize further the argument for the pristine nature of the high-Al basalts, we show they are compositionally distinct from known impact melts (Fig. 8). Of the many high-Al basalts analyzed by various authors, only three samples plot near known basaltic impact melt 14310. These are the matrix from KREEP breccia 14168, which is formed by impact activity, and the olivine vitrophyres 14321,1180 and 14321,1539 (Fig. 8) (Shervais et al. 1988; Neal and Taylor 1989), which have been shown to be impact melts (Neal et al. 2005). On the basis of these relationships, we conclude that the Apollo 14 high-Al mare basalts are pristine lunar volcanic products and not melts generated by meteorite impact, consistent with the conclusions of Ridley (1975), Warren et al. (1997), and Hagerty et al. (2001, 2002, 2003, 2005).

### "Groups" of Apollo 14 high-Al basalts

Elemental correlations of the Apollo 14 high-Al basalts define linear trends if only the REEs and/or other ITEs are plotted (see Fig. 2). Although this was modeled by 60% fractional crystallization and 13.2% KREEP assimilation ($r = 0.22$) by Neal et al. (1988, 1989b), such a linear trend also could be generated by simple two-component mixing between a low ITE basalt and KREEP, as could happen during an impact event (cf. Snyder et al. 2000; Snyder and Taylor 2000, 2001). It was Dasch et al. (1987) and Shih and Nyquist (1989a, 1989b) who showed a single event was not responsible for generating the Apollo 14 high-Al basalts (see Fig. 3). Kramer and Neal (2003) showed that simple element-element plots involving ITEs and compatible trace elements (CTEs) divide these basalts into three distinct compositional (and age) groups (Fig. 7) and modeled each group via a parent assimilating a KREEP component while undergoing fractional crystallization. This scenario was similar to the cyclic model proposed by Neal and Taylor (1990), but each parental basalt was derived by different degrees of partial melting of the

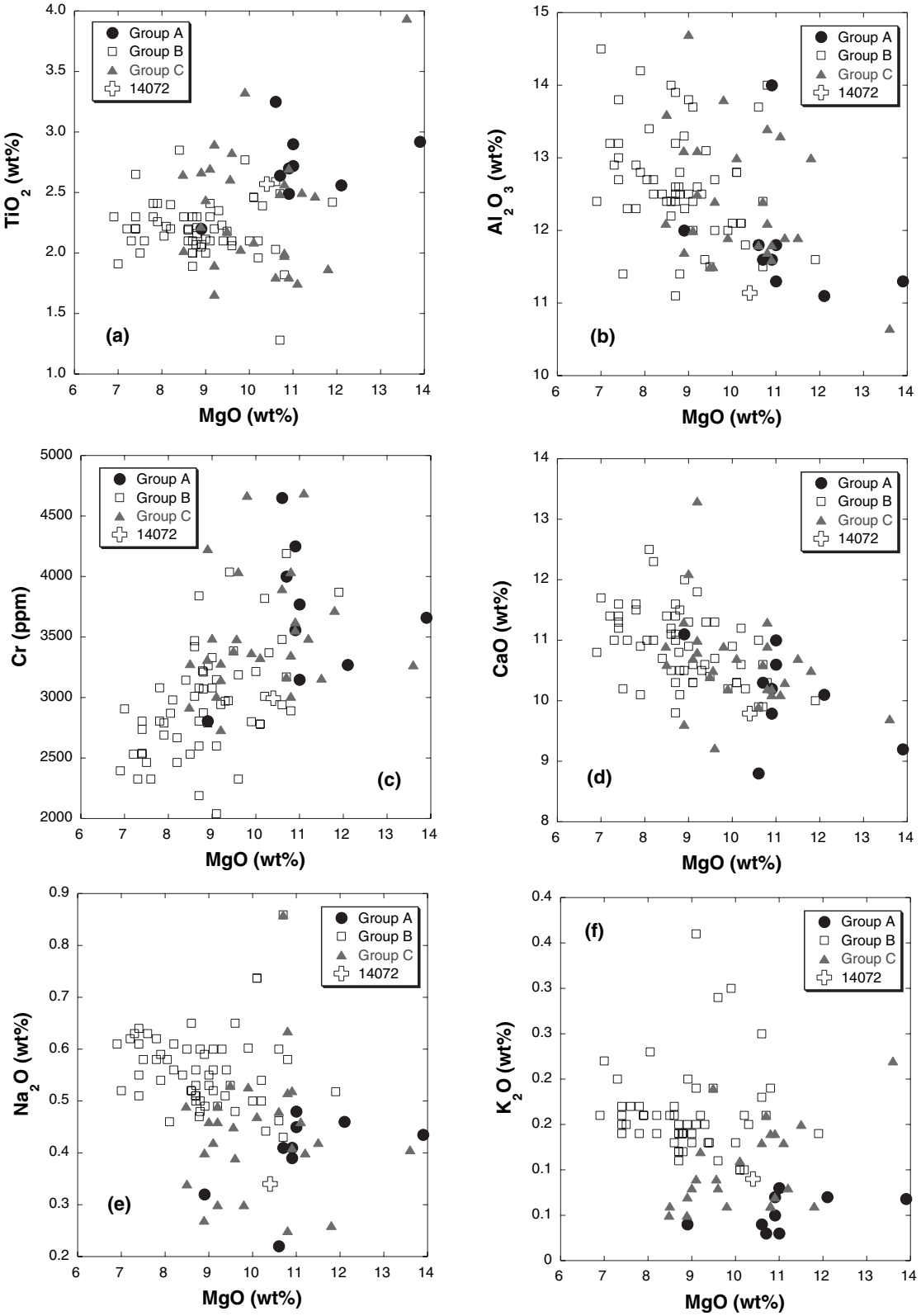


**FIGURE 6.** Major- and minor-element chemistry of the three groups of Apollo 14 high-Al basalts defined in this paper and 14072 plotted against MgO. Data sources are as in Figures 2 and 3.

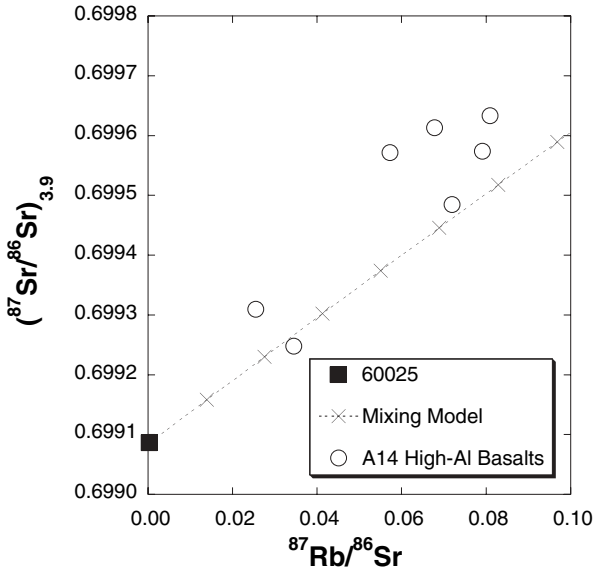


**FIGURE 7.** Mixing calculations using $^{87}Rb/^{86}Sr$ and $^{87}Sr/^{86}Sr$ to test the impact hypothesis for the generation of Apollo 14 high-Al basalts proposed by Snyder et al. (2000) and Snyder and Taylor (2000, 2001). The $^{87}Sr/^{86}Sr$ ratios of all data were recalculated to 3.9 Ga using the compositions of anorthosite 60025 (Carlson and Lugmair 1988), 15386 KREEP basalt (Nyquist et al. 1974), which was used in the calculations but for reasons of clarity is not plotted, and the Apollo 14 high-Al basalts from Papanastassiou and Wasserburg (1971), Compston et al. (1971, 1972), and Dasch et al. (1987). Tick marks on the mixing line represent 5% mixing increments.

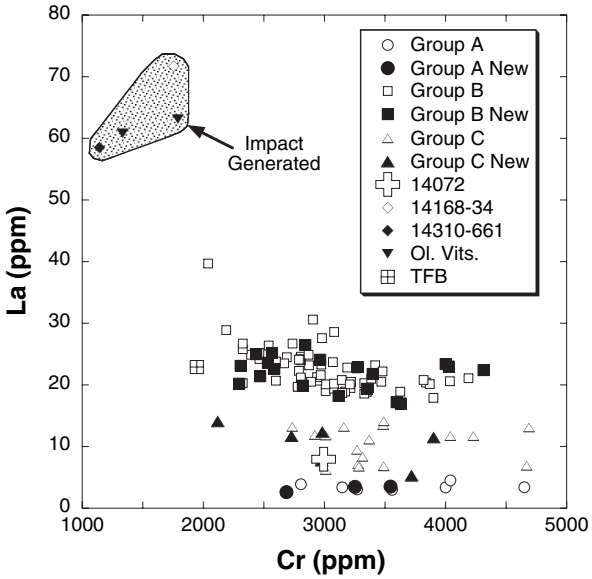


**FIGURE 8.** Plot of La vs. Cr for the Apollo 14 high-Al basalts depicting those samples analyzed in this study and comparing them with literature data. Sources of the published data are as in Figure 2. This simple element-element plot demonstrates the compositional distinction between the Apollo 14 high-Al basalts and impact-generated lithologies.

same source. Further examination has revealed that each group requires a separate source (Kramer and Neal 2005), as indicated by ITE ratios, and also consistent with the conclusions of Hagerty et al. (2005), which were based upon La/Yb ratios. For example, in Figure 9, ITE ratios are plotted using elements that do not substantially fractionate from each other during low-pressure (shallow) partial melting or fractional crystallization of the observed phenocryst phases in the Apollo 14 high-Al basalts. These elements have similar incompatibilities as observed on normalized element plots (see Fig. 4). Basalts with similar ratios of these elements would have been derived from a common source and three distinct groups are evident in Figure 9, where ratios of elements of similar incompatibility (e.g., Sun and McDonough 1989; McDonough and Sun 1995) are plotted. The groupings, by no coincidence, fall into the compositional/chronological groups outlined above and, unlike our previous interpretation (Kramer and Neal 2003), the diverse Nb/Ce and La/Ta values indicate there are three distinct source regions.

Basalt sample 14072 is a large (45 g) pristine high-Al mare basalt (El Goresy et al. 1972a, 1972b). Previously reported ITE compositions of 14072 (Neal 2001) would group it together with 14053 as a Group C basalt, although Dickinson et al. (1985) considered its ITE composition placed it within their Group 4 (our Group A). Strontium-isotopic data dates the sample at 4.00 ± 0.08 Ga with an $I_{Sr}$ of 0.69933 ± 7 (Dasch et al. 1987), and 3.99 ± 0.09 Ga with an $I_{Sr}$ of 0.69927 ± 7 (Compston et al. 1971). The age and $I_{Sr}$ for 14072 are within error of 14053 (Papanastassiou and Wasserburg 1971; Compston et al. 1972), but the Nb/Ce and La/Ta values for 14072 are intermediate between Groups A and C, such that 14072 is unlikely to share a common source with these two basalt groups (Fig. 9). Based on this evidence, we believe that 14072 may represent another high-Al group. However, due to the lack of other basalts of similar composition, we have not conducted quantitative modeling of this sample here.

## Petrogenetic modeling

The different groups of Apollo 14 high-Al basalts exhibit ranges in both trace-element abundance and in some trace-element ratios. Variations in some ITE ratios within the groups are difficult to generate through different degrees of partial melting of a common source, even if it was contaminated by urKREEP. For example, the Nb/Ce ratio of urKREEP is 0.357 (Warren and Wasson 1979), similar to the Group B basalts. Producing variations in this ratio through different degrees of partial melting would be difficult, as urKREEP, which would dominate the Nb and Ce abundances, would soon be exhausted in the source. Therefore, progressive melting of the source is required to dilute the urKREEP signature; however, because the residual source would contain much lower Nb and Ce abundances (and would have to have a higher Nb/Ce ratio), generating the Groups A and C basalts would require unfeasibly large degrees of partial melting (>25%). Therefore, we model the petrogenesis of the different high-Al basalt groups in terms of post-magma generation processes. To achieve this, parental compositions need to be defined for each group. This was done by creating a database of all basalt compositions within each group and defining elemental compatibility/incompatibility by plotting each element against a fractionation index (e.g., MgO, Cr, La). A hybrid parent composition can then be estimated by taking the lowest value for

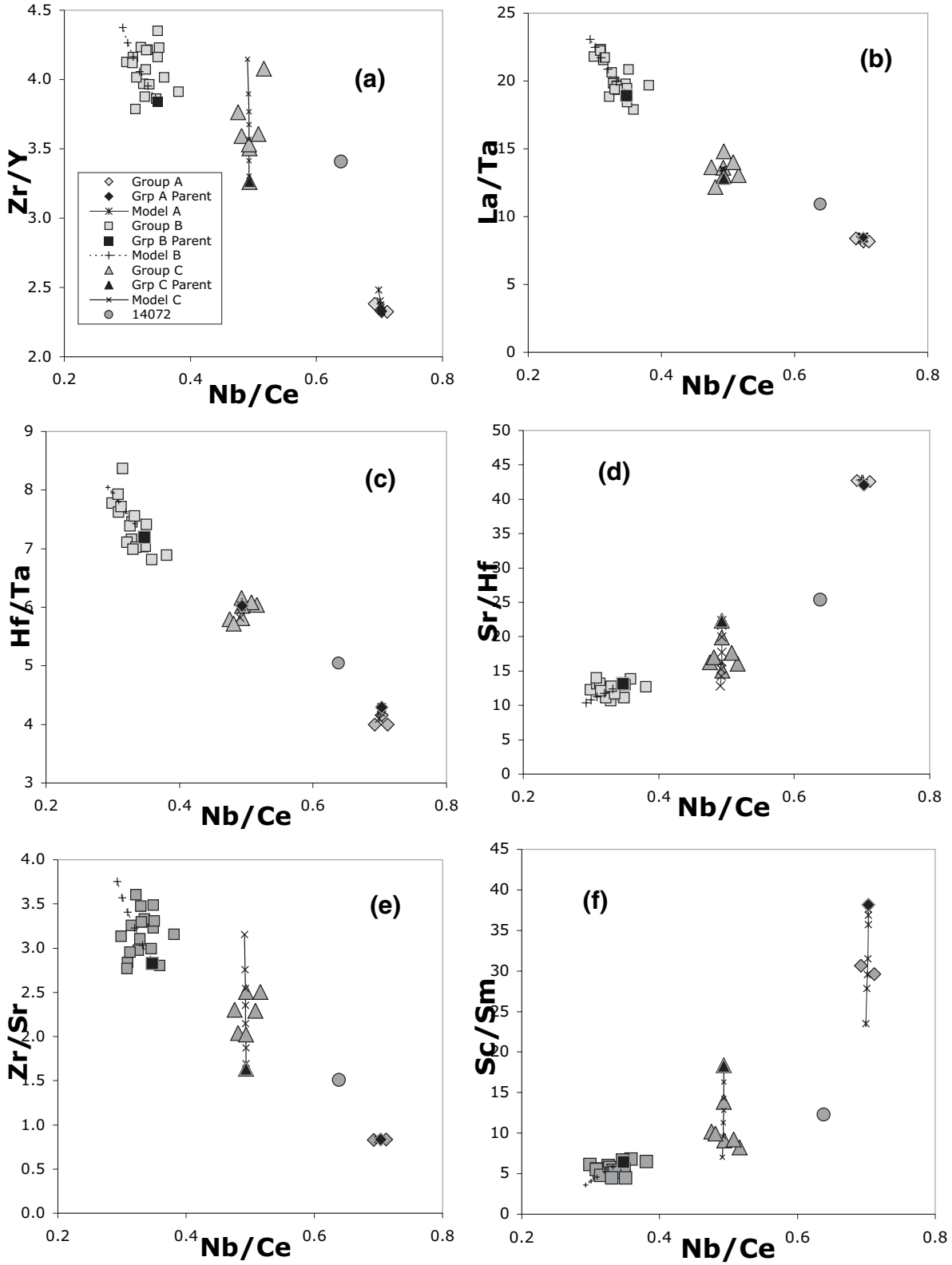


**FIGURE 9.** Ratio-ratio plots for the Apollo 14 high-Al basalts analyzed in this study. Also shown are the parental magma compositions for basalt group along with evolution pathways. Modeling parameters are given in Tables 2–5. See text for discussion.

each ITE and the highest value for each CTE (e.g., Cr, Ni, etc.). This procedure assumes that there has been no significant crystal accumulation, which is supported by petrography. The parental magma trace-element compositions for each group are given in Table 2. Although it is realized that these are only an estimate of parental compositions, they are used as a starting point for petrogenetic modeling.

**TABLE 2.** Parameters used in the modeling of the Apollo 14 high-Al basalts

| Partition Coefficients (Snyder et al. 1992; Green 1994): | | | | | | |
|---|---|---|---|---|---|---|
| | Olivine | Spinel | Plagioclase | Opx | Cpx | Pigeonite |
| Cr | 3 | 10 | 0.0332 | 5 | 5 | 5 |
| Co | 4 | 4 | 0.02 | 1.3 | 1.2 | 1.3 |
| Sc | 0.3 | 1.5 | 0.007 | 1.6 | 1.6 | 1.6 |
| Rb | 0.0001 | 0.001 | 0.08 | 0.023 | 0.025 | 0.003 |
| Sr | 0.0001 | 0.005 | 1.61 | 0.018 | 0.09 | 0.002 |
| Y | 0.006 | 0.006 | 0.027 | 0.2 | 0.5 | 0.2 |
| Zr | 0.013 | 0.06 | 0.013 | 0.063 | 0.156 | 0.063 |
| Nb | 0.0001 | 0.08 | 0.005 | 0.02 | 0.06 | 0.02 |
| Ba | 0.0001 | 0.001 | 0.686 | 0.013 | 0.013 | 0.013 |
| La | 0.0001 | 0.007 | 0.042 | 0.007 | 0.2 | 0.0009 |
| Ce | 0.0001 | 0.009 | 0.047 | 0.002 | 0.02 | 0.017 |
| Sm | 0.0006 | 0.009 | 0.017 | 0.022 | 0.17 | 0.011 |
| Eu | 0.0007 | 0.008 | 1.2 | 0.015 | 0.16 | 0.0068 |
| Yb | 0.019 | 0.009 | 0.007 | 0.17 | 0.4 | 0.087 |
| Lu | 0.03 | 0.02 | 0.007 | 0.22 | 0.3 | 0.11 |
| Hf | 0.013 | 0.05 | 0.013 | 0.063 | 0.3 | 0.063 |
| Ta | 0.01 | 0.06 | 0.005 | 0.01 | 0.06 | 0.01 |
| Th | 0.03 | 0.001 | 0.021 | 0.13 | 0.13 | 0.13 |

| Parental Melts | | | |
|---|---|---|---|
| | Group A | Group B | Group C |
| Cr | 4650 | 4313 | 4690 |
| Co | 45.4 | 41.5 | 48.7 |
| Sc | 61.1 | 56.0 | 60.0 |
| Rb | 0.80 | 1.97 | 0.99 |
| Sr | 56 | 85.0 | 56.5 |
| Y | 20.1 | 62.5 | 28.3 |
| Zr | 46.8 | 240 | 92.3 |
| Nb | 5.14 | 16.0 | 7.45 |
| Ba | 30.6 | 120 | 54.0 |
| La | 2.62 | 17.0 | 5.40 |
| Ce | 7.31 | 46.0 | 15.1 |
| Sm | 1.60 | 8.74 | 3.28 |
| Eu | 0.52 | 1.11 | 0.52 |
| Yb | 2.66 | 6.31 | 3.44 |
| Lu | 0.38 | 0.90 | 0.48 |
| Hf | 1.33 | 6.47 | 2.53 |
| Ta | 0.31 | 0.90 | 0.42 |
| Th | 0.36 | 1.30 | 0.70 |

The modeling of the Apollo 14 high-Al basalts is illustrated in Figure 9 by various trace element ratios that distinguish the different groups. Modeling parameters and results for selected elemental abundances are shown in Tables 3–5 where they are compared to the ranges within each group. Crystallization sequences were derived from a combination of petrographic observations and modeling using the MELTS program (e.g., Ghiorso and Sack 1995). The parameters used were as follows: starting pressure = 10 kbar; ending pressure = 1 kbar; starting temperature = 1350 °C. The program then was allowed to run until the magma had completely crystallized and starting oxygen fugacity = $-13.5 \log f_{O_2}$.

### Group A high-Al basalts

Unlike previous modeling of the Apollo 14 high-Al basalts, the Group A basalts do not require open-system evolution though assimilation of the KREEP component. The narrow ranges of ITE ratios (Figs. 9a–9e) indicate that closed-system fractional crystallization can generate the observed compositions. Although this conclusion may be a function of having Nb quantified in only three samples, we note that the average Hf/Ta ratio of previously analyzed Group A basalts (7 samples) is 4.2 ± 0.4 compared to 4.3 ± 0.2 for our new data. In addition, the average La/Ta ratio of previously analyzed Group A basalts is 7.5 (± 0.7) compared to 8.1 ± 0.4 for the new data. The Group A basalt compositions can be generated by 30–40% closed-system fractional crystallization, which includes the range in Sc/Sm (Fig. 9f) using the crystallization sequence and parameters defined in Tables 2 and 3.

### Group B high-Al basalts

The Group B high-Al basalts exhibit a range in ITE ratios (Figs. 9a–9e), but a relatively limited range is Sc/Sm (Fig. 9f). These data cannot be generated by closed-system fractional crystallization processes as this would produce limited variations in ITE ratios and moderate variations of Sc/Sm. KREEP assimilation models (Shervais et al. 1985; Dickinson et al. 1985; Neal et al. 1988, 1989b; Neal and Taylor 1990) also are inadequate to produce the observed ranges in ITE ratios observed for the Group B basalts because urKREEP and KREEP basalt 15386 have ITE ratios similar to these basalts. This would require un-

**TABLE 2.** —*Continued.* Evolved lithologies used in the modeling of the Apollo 14 high-Al basalts

| Sample no. | 14303,204[1] | 14321,1027[1] | 14161,7069[2] | 14161,7373[2] | Group B | Group C |
|---|---|---|---|---|---|---|
| Rock type | Granite | Granite | QMD | QMD | Assimilant | Assimilant |
| Cr | 550 | 17 | 361 | 982 | 516 | 208 |
| Co | 14.1 | 0.94 | 7.2 | 15 | 9.67 | 4.76 |
| Sc | 10.7 | 3 | 30.2 | 42.2 | 24.5 | 14.7 |
| Rb | 114 | 210 | 52 | 21 | 86.7 | 116 |
| Sr | 210 | 55 | 160 | 207 | 163 | 110 |
| Y | 204 | 201 | 7984 | 994 | 617 | 439 |
| Zr | 1020 | 660 | 4240 | 7150 | 3753 | 2128 |
| Nb | 57.1 | 144 | 161 | 75.3 | 111 | 142 |
| Ba | 2100 | 2160 | 2050 | 740 | 1689 | 2110 |
| La | 58 | 44.3 | 228 | 696 | 298 | 119 |
| Ce | 149 | 117 | 537 | 1683 | 719 | 288 |
| Sm | 22 | 15.9 | 96.5 | 326 | 134 | 48.8 |
| Eu | 3.3 | 1.17 | 3.35 | 5.68 | 3.60 | 2.26 |
| Yb | 18 | 32.2 | 74 | 146 | 76.0 | 47.5 |
| Lu | 2.6 | 5.1 | 10.2 | 18.7 | 10.2 | 6.89 |
| Hf | 21.6 | 13.9 | 100 | 163 | 86.0 | 49.1 |
| Ta | 3.3 | 8.3 | 9.2 | 4.3 | 6.37 | 8.16 |
| Th | 31 | 65 | 44 | 37 | 43.5 | 53.2 |

*Notes:* 1 = Warren et al. (1983); 2 = Jolliff (1991).

**TABLE 3.** Modeling results for Apollo 14 group A high-Al basalts

| Stage | 1 | 2 | 3 | 4 | 5 | 6 | 7 | 8 | Published |
|---|---|---|---|---|---|---|---|---|---|
| % Cryst. | 1 | 4 | 5 | 4 | 10 | 4 | 4 | 12 | Range* |
| Cumulative %FC | 1 | 5 | 10 | 14 | 24 | 28 | 32 | 44 | |
| Cr | 4551 | 4182 | 3736 | 3332 | 2329 | 1978 | 1680 | 1074 | 2686–4650 |
| Co | 44.1 | 39.0 | 33.9 | 31.3 | 27.9 | 27.6 | 27.3 | 26.9 | 27.0–45.4 |
| Sc | 61.5 | 63.4 | 65.3 | 65.9 | 64.5 | 62.9 | 61.4 | 58.0 | 45.0–70.1 |
| Rb | 0.81 | 0.84 | 0.89 | 0.92 | 1.02 | 1.07 | 1.11 | 1.26 | 0.80–1.49 |
| Sr | 56.6 | 58.9 | 62.0 | 64.6 | 71.7 | 74.6 | 77.5 | 85.7 | 56.0–77.7 |
| Y | 20.3 | 21.1 | 22.2 | 23.1 | 25.3 | 26.0 | 26.6 | 28.9 | 20.1–26.2 |
| Zr | 47.3 | 49.2 | 51.8 | 53.8 | 59.5 | 61.8 | 64.0 | 71.7 | 46.8–67.0 |
| Nb | 5.19 | 5.41 | 5.69 | 5.93 | 6.58 | 6.84 | 7.11 | 8.04 | 5.14–6.84 |
| Ba | 30.9 | 32.2 | 33.9 | 35.3 | 39.2 | 40.8 | 42.5 | 47.8 | 30.6–50.0 |
| La | 2.65 | 2.76 | 2.90 | 3.02 | 3.36 | 3.49 | 3.61 | 4.04 | 2.62–4.52 |
| Ce | 7.38 | 7.69 | 8.10 | 8.43 | 9.36 | 9.75 | 10.2 | 11.5 | 7.31–10.4 |
| Sm | 1.62 | 1.68 | 1.77 | 1.84 | 2.05 | 2.13 | 2.21 | 2.47 | 1.60–2.54 |
| Eu | 0.53 | 0.55 | 0.58 | 0.60 | 0.67 | 0.69 | 0.72 | 0.79 | 0.52–0.87 |
| Yb | 2.69 | 2.80 | 2.94 | 3.05 | 3.36 | 3.47 | 3.57 | 3.91 | 2.66–3.40 |
| Lu | 0.38 | 0.40 | 0.42 | 0.43 | 0.48 | 0.49 | 0.51 | 0.56 | 0.38–0.67 |
| Hf | 1.34 | 1.40 | 1.47 | 1.53 | 1.69 | 1.75 | 1.81 | 2.00 | 1.33–2.50 |
| Ta | 0.31 | 0.33 | 0.34 | 0.36 | 0.40 | 0.41 | 0.43 | 0.49 | 0.31–0.60 |
| Th | 0.36 | 0.38 | 0.40 | 0.41 | 0.45 | 0.47 | 0.49 | 0.55 | 0.36–0.55 |
| Crystallizing Assemblages (%): | | | | | | | | | |
| Olivine | 92 | 95 | 82 | 30 | 30 | | | | |
| Spinel | 8 | 5 | 3 | | | | | | |
| Plagioclase | | | | | | 10 | 10 | 10 | |
| Opx | | | 15 | 40 | 36 | | | | |
| Cpx | | | | | | 32 | 65 | 65 | |
| Pigeonite | | | | 30 | 34 | 58 | 25 | 25 | |

*Notes:* FC = Fractional Crystallization; Cryst. = Crystallized. Elemental data are in ppm.
* Published Range refers to the range of compositions reported previously in the literature and this work for the Group A basalts. See text for data sources.

**TABLE 4.** Modeling results for Apollo 14 Group B high-Al basalts

| Stage | 1 | 2 | 3 | 4 | 5 | 6 | 7 | Published |
|---|---|---|---|---|---|---|---|---|
| % Cryst. | 1 | 4 | 5 | 5 | 5 | 5 | 12 | Range* |
| Cumulative % FC | 1 | 5 | 10 | 15 | 20 | 25 | 37 | |
| Cr | 4187 | 3749 | 3234 | 2652 | 2175 | 1774 | 1069 | 2040–4313 |
| Co | 40.1 | 34.9 | 30.0 | 28.0 | 26.2 | 25.9 | 25.3 | 25.0–41.4 |
| Sc | 56.3 | 57.9 | 59.2 | 58.3 | 57.4 | 55.8 | 52.0 | 48.9–66.0 |
| Rb | 2.09 | 2.58 | 3.22 | 3.89 | 4.60 | 5.35 | 7.36 | 1.97–6.74 |
| Sr | 86.0 | 90.4 | 96.1 | 102 | 108 | 114 | 128 | 85–125 |
| Y | 63.8 | 69.3 | 76.4 | 83.4 | 90.7 | 97.5 | 114 | 62.5–97.5 |
| Zr | 247 | 274 | 310 | 247 | 387 | 427 | 533 | 251–450 |
| Nb | 16.3 | 17.5 | 19.0 | 20.7 | 22.4 | 24.2 | 29.0 | 16.0–24.5 |
| Ba | 123 | 136 | 153 | 171 | 190 | 209 | 260 | 120–216 |
| La | 17.5 | 19.6 | 22.4 | 25.3 | 28.4 | 31.5 | 39.6 | 17.0–39.7 |
| Ce | 47.3 | 52.6 | 59.5 | 66.9 | 75.6 | 82.6 | 104 | 46.0–105 |
| Sm | 8.98 | 9.97 | 11.3 | 12.7 | 14.1 | 15.6 | 19.4 | 8.74–17.6 |
| Eu | 1.13 | 1.19 | 1.27 | 1.36 | 1.45 | 1.53 | 1.74 | 1.01–1.67 |
| Yb | 6.46 | 7.07 | 7.87 | 8.68 | 9.53 | 10.4 | 12.5 | 6.26–12.2 |
| Lu | 0.92 | 1.01 | 1.11 | 1.22 | 1.34 | 1.46 | 1.75 | 0.90–1.59 |
| Hf | 6.63 | 7.30 | 8.18 | 9.09 | 10.0 | 11.0 | 13.4 | 6.47–11.5 |
| Ta | 0.92 | 0.98 | 1.07 | 1.17 | 1.26 | 1.37 | 1.65 | 0.87–1.44 |
| Th | 1.36 | 1.62 | 1.95 | 2.30 | 2.66 | 3.03 | 4.04 | 1.30–3.60 |
| Crystallizing Assemblages (%): | | | | | | | | |
| Olivine | 95 | 50 | 82 | 30 | 30 | | | |
| Spinel | 5 | 4 | 3 | | | | | |
| Plagioclase | | | | | | 10 | 10 | |
| Opx | | 41 | 15 | 40 | 36 | | | |
| Cpx | | | | | | 32 | 65 | |
| Pigeonite | | | | 30 | 34 | 58 | 25 | |

*Notes:* Elemental data are in ppm. FC = Fractional Crystallization; Cryst. = Crystallized.
* Published Range refers to the range of compositions reported previously in the literature and this work for the Group B basalts. See text for data sources.

feasibly large amounts of assimilation to generate the observed range of ITE ratios of the Group B basalts. Furthermore, it is difficult to model the range in ITE ratios through variable degrees of partial melting of a KREEP-rich source using conventional lunar mineralogy, as the ITE abundances and ratios would be controlled by the enriched mesostasis material (i.e., the first to melt) that would have KREEPy ITE ratios. The compositional range of these basalts can be generated through assimilation of a component that is a mixture of evolved compositions: KREEP-rich quartz monzodiorite (QMD) and granite. This combination of lithologies requires that there be a relationship between these two rock types. In fact, such a relationship was postulated by Ryder (1976). For the illustrative modeling presented here, the assimilant composition used for the Group B basalts was calculated from QMD compositions (14161,7069 and 14161,7373) reported by Jolliff (1991) and the lunar granite compositions (14303,204 and 14321,1027) reported by Warren et al. (1983) (Table 4) in the proportions 3:3:2:2. This combination of evolved lithologies

**TABLE 5.** Modeling results for Apollo 14 Group C high-Al basalts

| Stage | | 1 | 2 | 3 | 4 | 5 | 6 | 7 | Published |
|---|---|---|---|---|---|---|---|---|---|
| % Cryst. | | 1 | 3 | 5 | 4 | 4 | 5 | 10 | Range* |
| Cumulative % FC | | 1 | 4 | 9 | 13 | 17 | 22 | 32 | |
| | Cr | 4535 | 4154 | 3553 | 3085 | 2603 | 2028 | 1216 | 2120–4690 |
| | Co | 47.2 | 42.2 | 35.5 | 32.2 | 30.3 | 29.6 | 28.3 | 28.0–48.7 |
| | Sc | 60.4 | 61.6 | 63.2 | 63.5 | 62.5 | 59.9 | 54.7 | 55.0–64.5 |
| | Rb | 1.21 | 1.88 | 3.06 | 4.04 | 5.06 | 6.41 | 9.34 | 0.99–5.04 |
| | Sr | 57.3 | 59.6 | 63.8 | 67.2 | 70.8 | 75.4 | 85.4 | 56.5–105 |
| | Y | 29.4 | 32.7 | 38.4 | 43.1 | 47.8 | 53.4 | 64.9 | 28.3–64.5 |
| | Zr | 97.0 | 112 | 137 | 158 | 180 | 207 | 269 | 92.3–263 |
| | Nb | 7.78 | 8.79 | 10.6 | 12.1 | 13.6 | 15.6 | 20.0 | 7.45–19.6 |
| | Ba | 58.3 | 71.6 | 95.0 | 114 | 135 | 161 | 220 | 58.4–200 |
| | La | 5.67 | 6.49 | 7.94 | 9.15 | 10.4 | 12.0 | 15.5 | 5.32–15.3 |
| | Ce | 15.8 | 17.8 | 21.4 | 24.5 | 27.6 | 31.7 | 40.89 | 15.0–39.7 |
| | Sm | 3.40 | 3.77 | 4.42 | 4.96 | 5.52 | 6.25 | 7.79 | 3.28–7.59 |
| | Eu | 0.53 | 0.56 | 0.61 | 0.65 | 0.69 | 0.75 | 0.86 | 0.52–1.39 |
| | Yb | 3.56 | 3.93 | 4.56 | 5.09 | 5.62 | 6.29 | 7.66 | 3.44–6.66 |
| | Lu | 0.50 | 0.55 | 0.644 | 0.71 | 0.79 | 0.89 | 1.09 | 0.48–0.97 |
| | Hf | 2.64 | 2.99 | 3.60 | 4.11 | 4.63 | 5.28 | 6.67 | 2.53–6.53 |
| | Ta | 0.44 | 0.50 | 0.60 | 0.68 | 0.77 | 0.89 | 1.15 | 0.40–1.14 |
| | Th | 0.80 | 1.12 | 1.67 | 2.12 | 2.59 | 3.19 | 4.53 | 0.70–2.00 |
| Crystallizing assemblages (%): | | | | | | | | | |
| Olivine | | 90 | 95.6 | 86.5 | 60 | 30 | | | |
| Spinel | | 10 | 4.4 | 3.5 | | | | | |
| Plagioclase | | | | | | | | | |
| Opx | | | | 10 | 40 | 36 | | | |
| Cpx | | | | | | | 32 | 65 | |
| Pigeonite | | | | | | 34 | 68 | 35 | |

*Notes:* FC = Fractional Crystallization; Cryst. = Crystallized.
* Published Range refers to the range of compositions reported previously in the literature and this work for the Group C basalts. See text for data sources.

adequately models the ITE ratios shown in Figure 9. To use these compositions in the modeling of Group B (and Group C) high-Al basalts, Nb and Y had to be estimated. Niobium was estimated using the published Ta values and assuming a chondritic Nb/Ta ratio of 17.3 (Anders and Grevesse 1989; Sun and McDonough 1989) for the sample. Yttrium abundances were estimated from Dy abundances, assuming that the chondrite-normalized value of Dy was that of Y and converting this to ppm Y using a chondritic value of 1.565 (Anders and Grevesse 1989; Sun and McDonough 1989). The AFC model (Depaolo 1981) was calculated using 0.1 as the *r* value (mass assimilated:mass crystallized) and the trends defined by the Group B high-Al basalts are generated by 25% fractional crystallization and 2.5% assimilation (Figs. 9a–9f). Table 4 shows that the ranges in elemental abundances for the Group B, high-Al basalts (from this work and the literature where applicable) are also generated by this model. Note that the assimilant composition is calculated from components that have been found at the Apollo 14 site.

### Group C high-Al basalts

The Group C high-Al basalts show a more limited range in ITE ratios compared to those of Group B, except for Zr/Y and Sc/Sm (Figs. 9a–9f). As with the Group B basalts, those of Group C cannot be explained by closed-system fractional crystallization processes or assimilation of KREEP. In fact, the Group C basalts require an assimilant composed of the same components as for the Group B basalts, namely granite (14303,204 and 14321,1027; Warren et al. 1983) and the QMD component represented only by 14161,7069 (Jolliff 1991) in the proportions of 1:5:4 (Table 5). The range of Group C basalts can be generated by 40% fractional crystallization accompanied by 4.8% assimilation (*r* = 0.12). Although there is some discrepancy in the amount of AFC required to generate the array of data (e.g., compare Fig. 9a with Fig. 9c), we are using published compositions of evolved lithologies to generate our assimilant as an illustration that the Group C basalts evolved through open-system processes. Table 5 shows that the ranges of elemental abundances for the Group C high-Al basalts (from this work and the literature where applicable) are also generated by this model.

### Limitations

The petrogenetic models presented above and in Tables 2–5 and Figure 9 generate the range of trace-element ratios displayed by each group as well as the ranges in abundances for the majority of elements (see Tables 3–5). However, although the range in Sc/Sm ratio is modeled (Fig. 9f) the range in Sc abundances in Group A and Group B basalts is not (Tables 3 and 4). Samples with the lowest abundances for Group A (45 ppm in 14321,1530 and 51.9 ppm in 14321,1546; abundances determined by INA) plot to the left of the bulk of the Group A basalts and the model evolutionary path in Figure 10. For Group B basalts, the Sc data show a wider range than the model pathway and the samples do not form coherent trends in Figure 10. Although the range in Sc abundances for Group C basalts is generated by the AFC model presented here, these samples also do not form a coherent trend in Figure 10; however, the basalts analyzed in this study do closely follow the model evolution path. Four explanations are proposed for the Sc data in the Apollo 14 high-Al basalts: (1) If the model abundances for Sc are simply compared to the range observed for each basalt group, it could be argued that the partition coefficients for Sc may be incorrect. (2) The scatter in Figure 10 suggests the samples may reflect short-range unmixing of the main Sc carrier, pyroxene. Although Hagerty et al. (2001, 2002, 2003, 2005) concluded the Apollo 14 high-Al basalts were

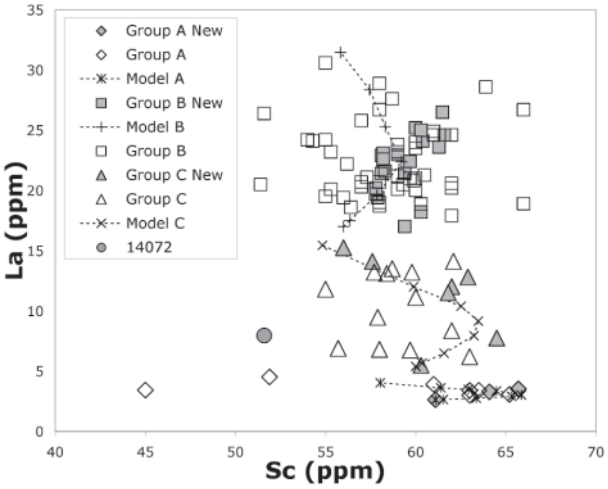


**FIGURE 10.** Plot of La vs. Sc for the Apollo 14 high-Al basalts depicting those samples analyzed in this study and comparing them with literature data. The considerable scatter in Sc is an anomaly compared to the other compatible elements. See text for discussion.

representative whole-rock analyses, their study only included trace-element analyses of olivine and plagioclase, and not the main carrier of Sc, namely pyroxene (although it seems unlikely that only pyroxene would exhibit short-range unmixing). (3) The Sc data used here are predominantly determined by INA and the scatter may, although unlikely, reflect imprecision for this element. Unfortunately, as noted above, during this study, the ICP-MS analysis of Sc suffered from a molecular interference on monoisotopic Sc. This was only recognized after the analyses were completed and the effect of the interference could not be corrected for. (4) The scatter in Figure 10 may be a product of multiple melting events during the generation of each basalt type and these melts followed similar, overlapping petrogenetic pathways for most elements. The scatter in the Sc data, especially for the Group B basalts, could have been produced by variable contributions from pyroxene in the source, as a fractionating phase, and/or the assimilant (possibly at different pressures) as each melt batch evolved. At this time, it is difficult to distinguish among these four explanations for the Sc data. The behavior of Sc during the petrogenesis of the Apollo 14 high-Al basalts remains a subject of future research.

Even though our modeling of the new data, despite its complexity, does not take into account every detail that would be necessary to produce a perfect representation of each Apollo 14 high-Al basalt group (e.g., partition coefficients used in the model would not, in reality, be constant throughout magmatic evolution), it does highlight significant advances from previous modeling. For example, modeling of the new data shows that Group A basalts evolved in a closed-system magma chamber, whereas the Group B and C basalts require an assimilant composed of a mixture of urKREEP (cf. Warren and Wasson 1979) and granite. It is also evident that, from the new data, the basalts consistently break into three distinct groups on the basis of age, ITE vs. CTE relationships, and ITE ratios that characterize the source. This new work clearly demonstrates that the Apollo 14 high-Al basalts were derived from at least three separate source regions at three separate times during the history of the Moon. In addition, the new data support an endogenous igneous origin for the Apollo 14 high-Al basalts rather than formation through impact melting.

**TABLE 6.** Average compositional data for each of the groups of Apollo 14 high-Al basalts

| | Group A | 14072 | Group C | Group B |
|---|---|---|---|---|
| $TiO_2$ (wt%) | 2.64 | 2.57 | 2.46 | 2.20 |
| $Al_2O_3$ | 11.8 | 11.1 | 12.5 | 12.6 |
| FeO | 17.9 | 17.8 | 16.6 | 16.4 |
| MgO | 11.1 | 12.2 | 10.0 | 9.1 |
| CaO | 10.1 | 9.79 | 10.7 | 10.8 |
| $Na_2O$ | 0.38 | 0.34 | 0.44 | 0.44 |
| $K_2O$ | 0.05 | 0.09 | 0.1 | 0.16 |
| ***Mg*** | 0.524 | 0.550 | 0.519 | 0.497 |
| Sc (ppm) | 63.6 | 51.6 | 60.7 | 59.4 |
| V | 139 | 104 | 125 | 117 |
| Cr | 3355 | 2994 | 3137 | 3088 |
| Co | 37.2 | 39.7 | 39.2 | 34.1 |
| Ga | 3.9 | 5.2 | 4.4 | 5.7 |
| Rb | 1.13 | 1.55 | 2.14 | 3.23 |
| Sr | 65.3 | 93.4 | 85.0 | 100.2 |
| Y | 23.2 | 41.4 | 51.7 | 77.9 |
| Zr | 54.3 | 141 | 189 | 317 |
| Nb | 6.02 | 12.9 | 14.8 | 19.8 |
| Ba | 35.9 | 107 | 120 | 167 |
| La | 3.14 | 7.96 | 11.3 | 22.4 |
| Ce | 8.57 | 20.2 | 29.8 | 59.5 |
| Sm | 1.97 | 4.21 | 5.74 | 11.0 |
| Eu | 0.59 | 0.98 | 0.91 | 1.30 |
| Yb | 2.88 | 4.01 | 5.58 | 7.75 |
| Lu | 0.44 | 0.59 | 0.81 | 1.10 |
| Hf | 1.54 | 3.68 | 4.95 | 8.15 |
| Ta | 0.38 | 0.73 | 0.84 | 1.11 |
| Th | 0.47 | 1.02 | 1.59 | 2.36 |
| Nb/Ce | 0.703 | 0.639 | 0.495 | 0.332 |
| La/Ta | 8.26 | 10.9 | 13.5 | 20.1 |
| Hf/Ta | 4.04 | 5.04 | 5.92 | 7.34 |
| Zr/Y | 2.34 | 3.41 | 3.66 | 4.07 |
| Zr/Sr | 0.833 | 1.51 | 2.23 | 3.16 |
| Sr/Hf | 42.5 | 25.4 | 17.2 | 12.3 |
| Sc/Sm | 32.3 | 12.3 | 10.6 | 5.4 |
| Rb/Sr | 0.0173 | 0.0166 | 0.0252 | 0.0322 |

*Notes:* Major-element averages calculated from literature values (Shervais et al. 1985; Dickinson et al. 1985; Neal et al. 1988, 1989b). 14072 major-element data are from Hubbard et al. (1972). Trace-element averages calculated using the data in Table 1.

## Source region implications

The origin of the high-Al mare basalts has been under debate for 30 years (e.g., Ridley 1975; Kurat et al. 1976; Ma et al. 1979; Dickinson et al. 1985; Shervais et al. 1985; Neal et al. 1988, 1989a, 1989b; Kramer and Neal 2003, 2005; Hagerty et al. 2001, 2002, 2003, 2005). For example, one question that is still under debate concerns the origin of the "high-Al" nature of these basalts (relative to other mare basalts): is the high-Al nature due to a source characteristic or is it inherited by assimilation of the anorthositic lunar crust? Finnila et al. (1994) demonstrated that the temperature at the crust-mantle interface is too low for plagioclase assimilation to occur in sufficient quantity to impart the high-Al signature to a lunar basaltic magma. This supports the notion that the aluminous nature of these basalts is a source feature. However, recent work by Liang et al. (2005) suggested that instead of assimilation and fractional crystallization (cf. Finnila et al. 1994), the high-Al basalts can be modeled by a mechanism

of anorthite dissolution. These authors used phase diagrams to argue that anorthosite can be dissolved by a superheated picritic mare magma, and that this would impart the high-Al nature to these basalts without any accompanying crystallization. As this can be modeled as simple two-component mixing, it was tested by conducting a simple mixing calculation for the major- and trace-element compositions using an average Apollo 15 olivine-normative mare basalt (e.g., Ryder and Schuraytz 2001) as the magmatic end-member and three different anorthositic end-members: 14321,1273 (Mg-Suite); 15455c (Mg-Suite) (Ryder 1985; Heiken et al. 1991); 60015 (FAN) (Ryder and Norman 1980; Heiken et al. 1991). Although our simplistic modeling can generate the major-element compositions of the high-Al basalts through dissolution of 10–20% of the anorthosites, the trace-element abundances are too low. Each contaminant composition is required to be a 80:20 anorthosite:urKREEP (Warren 1988) mixture to generate the trace-element abundances. Unfortunately, such a mixture has difficulty in generating the ITE ratios of the Apollo 14 high-Al basalts. Therefore, we suggest that assimilation (or dissolution) of crustal materials is not responsible for the high-Al nature of the Apollo 14 mare basalts studied here and that this signature has been imparted from each source region.

The Apollo 14 high-Al basalts exhibit ranges in ITE ratios (and abundances) that exhibit some regularity in the distribution of the different groups. There is a decrease in ITE abundances between the groups in the order B → C → A, which correlates negatively with Nb/Ce, Sr/Hf, and Sc/Sm, and correlates positively with La/Ta, Hf/Ta, and Zr/Sr (Table 6). In addition, if average major-element abundances are calculated, there is a decrease in $Na_2O$ and $K_2O$, but an increase in $TiO_2$ in the order B → C → A (Table 6). A parental melt for each group would need to be derived from a source region that would have a distinct composition. The implications for source compositions are as follows: (1) if it is assumed that the ITE abundances are controlled by KREEP (cf. Hughes et al. 1990), this source component increases in the order A → C → B and is consistent with the average $Na_2O$ and $K_2O$ contents (Table 6); and (2) The variations in ITE ratios in the parental magmas (Fig. 9) are controlled by mineralogic variations in the source. A varying contribution of ilmenite in the source regions of the Apollo 14 high-Al basalts would produce variations in the above ratios. This is consistent with the increasing $TiO_2$ content of the average compositions (in the order B → C → A; Table 6). Although these averages overlap when the standard deviation is considered, they demonstrate subtle distinctions in the geochemistry of the high-Al basalts from each group. Furthermore, the $TiO_2$ distinctions also show a general positive correlation with ***Mg*** (Table 6). A negative correlation would be expected if the variation in Ti content were due to increased fractionation of a basaltic magma.

## Concluding remarks

The Apollo 14 high-Al basalts are not impact melts. The plots of CTEs vs. ITEs (Fig. 8) show a clear distribution of most of the basalts into three groups originating from three different sources and melting events, and eloquently demonstrates the compositional distinction between the high-Al basalts and known impact-generated samples from the Apollo 14 site. Coupled with the relatively siderophile-element-poor nature of high-Al basalts (Warren et al. 1997) and isotope systematics that are inconsistent with mixing between FAN crust and meteoritic material, the evidence that these rocks represent magmas derived by internal lunar processes is compelling. Using ratios of ITEs obtained by ICP-MS and heretofore not quantified for these samples, the Apollo 14 high-Al basalt suite can be shown to have been formed by at least three separate magmatic events that tapped compositionally distinct source regions. Chondrite-normalized trace-element profiles indicate that clinopyroxene was left in the residue, as indicated by a ubiquitous slight negative Y anomaly (Figs. 5a–5c). Integration of major- and trace-element chemistry indicates that, relatively speaking, the source regions for each basalt group exhibit an increase in KREEP component and decrease in ilmenite in the order A → C → B.

## Acknowledgments

This research was supported by NASA Cosmochemistry grant NAG5-12982 to CRN. Many thanks to Jinesh Jain, Will Kinman, and John Shafer for help with the ICP-MS analytical work. Thorough, thoughtful, and insightful reviews by Scott Hughes and Justin Hagerty improved the quality of this paper and are gratefully acknowledged.

## References cited

Albee, A.L., Chodos, A.A., Gancarz, A.J., Haines, E.L., Papanastassiou, D.A., Ray, L., Tera, F., Wasserburg, G.J., and Wen, T. (1972) Mineralogy, petrology, and chemistry of a Luna 16 basaltic fragment, sample B-1. Earth and Planetary Science Letters, 13, 353–367.

Anders, E. and Grevesse, N. (1989) Abundances of the elements: Meteoritic and solar. Geochimica et Cosmochimica Acta, 53, 197–214.

Brown, R. (1977) A sample fusion technique for whole rock analysis with the electron microprobe. Geochimica et Cosmochimica Acta, 41, 435–438.

Brunfelt, A.O., Heier, K.S., Nilssen, B., Sundvoll, B., and Steiennes, E. (1972) Distribution of elements between different phases of Apollo 14 rocks and soils. Proceedings of the 3rd Lunar Science Conference, 2, 1133–1147.

Carlson, R.W. and Lugmair, G.W. (1988) The age of ferroan anorthosite 60025: Oldest crust on a young Moon? Earth and Planetary Science Letters, 90, 119–130.

Chazey, W.C., III, Neal, C.R., Jain, J., and Kinman, W.S. (2003) A reappraisal of Rb, Y, Zr, Pb, and Th values in geochemical reference material BHVO-1. Geostandards Newsletter, 27, 181–192.

Compston, W., Vernon, M.J., Berry, H., and Rudowski, R. (1971) The age of the Fra Mauro formation: A radiometric older limit. Earth and Planetary Science Letters, 12, 55–58.

Compston, W., Vernon, M.J., Berry, H., Rudowski, R., Chappell, B.W., and Kaye, M. (1972) Apollo 14 mineral ages and the thermal history of the Fra Mauro formation. Proceedings of the 3rd Lunar Science Conference, 2, 1487–1501.

Dasch, E., Shih, C.-Y., Bansal, B.M., Weismann, H., and Nyquist, L.E. (1987) Isotopic analysis of basaltic fragments from lunar breccia 14321: Chronology and petrogenesis of pre-imbrium mare volcanism. Geochimica et Cosmochimica Acta, 51, 3241–3254.

DePaolo, D. (1981) Trace element and isotopic effects of combined wallrock assimilation and fractional crystallization. Earth and Planetary Science Letters, 53, 189–202.

Dickinson, T., Taylor, G.J., Keil, K., Schmitt, R.A., Hughes, S.S., and Smith, M.R. (1985) Apollo 14 aluminous mare basalts and their possible relationship to KREEP. Proceedings of the 15th Lunar Science Conference, in Journal of Geophysical Research, 90, C365–C375.

Duncan, A.R., McKay, S.M., Stoeser, J.W., Lindstrom, M.M., Lindstrom, D.J., Fruchter, J.S., and Goles, G.G. (1975) Lunar polymict breccia 14321: A compositional study of its principal components. Geochimica et Cosmochimica Acta, 39, 247–260.

El Goresy, A., Ramdohr, P., and Taylor, L. (1972a) Fra Mauro crystalline rocks: petrology, geochemistry, and subsolidus reduction of the opaque minerals. Lunar Sci., III, 224–226 (abstr.). Lunar Science Institute, Houston.

El Goresy, A., Taylor, L.A., and Ramdohr, P. (1972b) Fra Mauro crystalline rocks: Mineralogy, geochemistry, and subsolidus reduction of the opaque minerals. Proceedings of the Third Lunar Science Conference, Supplement 3, Geochimica et Cosmochimica Acta, vol. 1, 333–349.

Finnila, A., Hess, P., and Rutherford, M. (1994) Assimilation by lunar mare basalts: Melting of crustal material and dissolution of anorthosite. Journal of Geophysical Research, 99, 14677–14690.

Ghiorso, M.S. and Sack, R.O. (1995) Chemical mass transfer in magmatic processes IV. A revised and internally consistent thermodynamic model for the interpola-

tion of liquid-solid equilibria in magmatic systems at elevated temperatures and pressures. Contributions to Mineralogy and Petrology, 119, 197–212.
Green, D.H., Ringwood, A.E., Ware, N.G., and Hibberson, W.O. (1972) Experimental petrology and petrogenesis of Apollo 14 basalts. Proceedings of the 3rd Lunar Science Conference, 2, 197–206.
Green, T.H. (1994) Experimental studies of trace-element partitioning applicable to igneous petrogenesis—Sedona 16 years later. Chemical Geology, 117, 1–36.
Grieve, R.A., McKay, G.A., and Weill, D.F. (1972) Microprobe studies of three Luna 16 basalt fragments. Earth and Planetary Science Letters, 13, 233–242.
——— (1975) Lunar polymict breccia 14321: A petrographic study. Geochimica et Cosmochimica Acta, 39, 229–245.
Hagerty, J., Shearer, C.K., and Papike, J.J (2001) Trace element variability of the Apollo 14 high-Al basalts. A result of igneous processes or sample size? Lunar and Planetary Science, XXXII, abstract 1235 (CD-ROM). Lunar and Planetary Institute, Houston.
——— (2002) Using small basaltic lunar clasts to reconstruct the early magmatic history of the Moon. Workshop on the Moon Beyond 2002, abstract 3041. Lunar and Planetary Institute, Houston.
——— (2003) Trace element characteristics of minerals in the Apollo 14 high-al basalts: Implications for an igneous versus an impact origin. Lunar and Planetary Science, XXXIV, abstract 1773 (CD-ROM). Lunar and Planetary Institute, Houston.
——— (2005) Trace element characteristics of the Apollo 14 high-alumina basalts: Implications for early magmatism on the Moon. Geochimica et Cosmochimica Acta, 69, 5831–5845.
Haskin, L.A. and Korotev, R. (1977) Test of a model for trace-element partitioning during closed system solidification of a silicate liquid. Geochimica et Cosmochimica Acta, 41, 921–939.
Head, J. and Wilson, L. (1992) Lunar mare volcanism: Stratigraphy, eruption conditions, and the evolution of secondary crusts. Geochimica et Cosmochimica Acta, 56, 2155–2175.
Heiken, G., Vaniman, D.T, and French, B.M., Eds. (1991) Lunar Sourcebook. Cambridge University Press, New York.
Helmke, P. and Haskin, L.A. (1972) Rare earths and other trace elements in Luna 16 soil. Earth and Planetary Science Letters, 13, 441–443.
Helmke, P., Haskin, L.A., Korotev, R., and Ziege, K. (1972) Rare earth and other trace elements in Apollo 14 samples. Proceedings of the 3rd Lunar Science Conference, 2, 1275–1292.
Hubbard, N.J., Gast, P., Rhodes, J.M., Bansal, B.M., and Weismann, H. (1972) Nonmare basalts: Part II. Proceedings of the 3rd Lunar Science Conference, 2, 1161–1179.
Hubbard, N.J., Rhodes, J., Wiesmann, H., Shih, C.-Y., and Bansal, B.M. (1974) The chemical definition and interpretation of rock types returned from the non-mare regions of the Moon. Proceedings of the 5th Lunar Science Conference, 2, 1227–1246.
Hughes, S.S., Neal, C.R., and Taylor, L.A. (1990) Petrogenesis of Apollo 14 high alumina (HA) parental basaltic magma. Lunar and Planetary Science, XX, 540–541 (abstract). Lunar and Planetary Institute, Houston.
Jackson, S., Longerich, H., and Horn, I. (1997) The application of laser ablation microprobe-inductively coupled plasma-mass spectrometry (LAMICP-MS) to in situ trace-element determinations in minerals. 4th Australian Symposium on Applied ICP-Mass Spectrometry, MacQuarie University, Sydney.
Jenner, G., Longerich, H., Jackson, S., and Fryer, B. (1990) ICP-MS: A powerful tool for high-precision trace-element analysis in earth sciences: Evidence from analysis of selected USGS reference samples. Chemical Geology, 83, 133–148.
Jolliff, B.L. (1991) Fragments of Quartz Monzodiorite and Felsite in Apollo 14 soil particles. Proceedings of the 21st Lunar Science Conference, 101–118.
Kramer, G.Y. and Neal, C.R. (2003) Petrogenesis of the Apollo 14 high-al basalts revisited: Distinct magmatic events, source metasomatism, and AFC. Lunar and Planetary Science, XXXIV, abstract 2035 (CD-ROM). Lunar and Planetary Institute, Houston.
——— (2005) Investigating the sources of the Apollo 14 high alumina mare basalts. Lunar and Planetary Science, XXXVI, abstract 1957 (CD-ROM). Lunar and Planetary Institute, Houston.
Kurat, G., Kracher, A., Keil, K., Warner, R.D., and Prinz, M. (1976) Composition and origin of Luna 16 aluminous mare basalts. Proceedings of the 7th Lunar Science Conference, 2, 1301–1321.
Liang, Y., Morgan, Z., and Hess, P. (2005) On the physical and chemical consequences of lunar picritic magma-anorthosite reaction. Lunar and Planetary Science, XXXVI, abstract 1706 (CD-ROM). Lunar and Planetary Institute, Houston.
Lindstrom, M.M. and Haskin, L.A. (1978) Causes of compositional variations within mare basalt suites. Proceedings of the Lunar Science Conference, 9th 465-486.
Longhi, J., Walker, D., and Hays, J.F. (1972) Petrography and crystallization history of basalts 14310 and 14072. Proceedings of the 3rd Lunar Science Conference, 2, 131–139.
Ma, M.-S., Schmitt, R.A., Nielsen, R., Taylor, G.J., Warner, R.D., and Keil, K. (1979) Petrogenesis of Luna 16 aluminous mare basalts. Geophysical Research Letters, 6, 909–912.
McDonough, W.F. and Sun, S.-S. (1995) The composition of the Earth. Chemical Geology, 120, 223–253.
Morgan, J., Laul, J., Krahenbuhl, U., Ganapathy, R., and Anders, E. (1972) Major impacts on the Moon: Characterization from trace elements in Apollo 12 and 14 samples. Proceedings of the 3rd Lunar Science Conference, 2, 1377–1395.
Neal, C.R. (2001) Interior of the Moon: The presence of garnet in the primitive deep lunar mantle. Journal of Geophysical Research, 106, 27865–27885.
Neal, C.R. and Kramer, G.Y. (2003) The composition of KREEP: A detailed study of KREEP basalt 15386. Lunar and Planetary Science, XXXIV, abstract 1665 (CD-ROM). Lunar and Planetary Institute, Houston.
Neal, C.R. and Taylor, L.A. (1989) Metasomatic products of the lunar magma ocean: The role of KREEP dissemination. Geochimica et Cosmochimica Acta, 53, 529–541.
——— (1990) Model of lunar basalt petrogenesis: Sr isotope evidence from Apollo 14 high-alumina basalts. Proceedings of the 20th Lunar Science Conference, 101–108.
——— (1992) Petrogenesis of mare basalts: A record of lunar volcanism. Geochimica et Cosmochimica Acta, 56, 2177–2211.
Neal, C.R., Taylor, L.A., and Lindstrom, M.M. (1988) Apollo 14 mare basalt petrogenesis: Assimilation of KREEP-like components by a fractionating magma. Proceedings of the 18th Lunar Science Conference, 139–153.
Neal, C.R., Taylor, L.A., and Patchen, A. (1989a) High alumina (HA) and very high potassium (VHK) basalt clasts from Apollo 14 breccias, part 1: Mineralogy and petrology: Evidence of crystallization from evolving magmas. Proceedings of the 19th Lunar Science Conference, 137–145.
Neal, C.R., Taylor, L.A., Schmitt, R.A., Hughes, S.S., and Lindstrom, M.M. (1989b) High alumina (HA) and very high potassium (VHK) basalt clasts from Apollo 14 breccias, part 2: Whole rock chemistry: Further evidence for combined assimilation and fractional crystallization within the lunar crust. Proceedings of the 19th Lunar Science Conference, 147–161.
Neal, C.R., Shearer, C.K., and Kramer, G.Y. (2005) Are the Apollo 14 high-Al basalts really impact melts? Lunar and Planetary Science, XXXVI, abstract 2023. Lunar and Planetary Institute, Houston.
Nyquist, L.E. and Shih, C.-Y. (1992) The isotopic record of lunar volcanism. Geochimica et Cosmochimica Acta, 56, 2213–2234.
Nyquist, L.E., Bansal, B.M., Wiesmann, H., and Jahn, B.-M. (1974) Taurus-littrow chronology: Some constraints on early lunar crustal development. Proceedings of the 5th Lunar Science Conference, 2, 1515–1539.
Papanastassiou, D.A. and Wasserburg, G.J. (1971) Rb-Sr ages of the igneous rocks from the Apollo 14 mission and the age of the Fra Mauro Formation. Earth and Planetary Science Letters, 12, 36–48.
——— (1972) Rb-Sr age of a Luna 16 basalt and the model age of lunar soils. Earth and Planetary Science Letters, 13, 368–374.
Papike, J.J. and Vaniman, D.T. (1978) The lunar mare basalt suite. Geophysical Research Letters, 5, 433–436.
Papike, J.J., Hodges, F.N., Bence, A.E., Cameron, M., and Rhodes, J.M. (1974) Mare basalt: Crystal chemistry, mineralogy, and petrology. Reviews of Geophysics and Space Physics, 14, 475–540.
Pearce, N., Perkins, W., Westgate, J., Gorton, M., Jackson, S., Neal, C.R., and Chenery, S. (1997) A compilation of new and published major and trace element data for NIST SRM612 glass reference materials. Geostandards Newsletter, 21, 115–144.
Rhodes, J.M. and Hubbard, N.J. (1973) Chemistry, classification, and petrogenesis of Apollo 15 mare basalts. Proceedings of the 4th Lunar Science Conference, 4, 1127–1148.
Ridley, W.I. (1975) On high-alumina mare basalts. Proceedings of the 6th Lunar Science Conference, 1, 131–145.
Ringwood, A.E., Green, D.H., and Ware, N. (1972) Experimental petrology and petrogenesis of Apollo 14 basalts. Lunar Sci., III, 654–656 (abstract). Lunar Science Institute, Houston.
Rose, H.J., Cuttitta, F., Annell, C.S., Carron, M.K., Christian, R.P., Dwornik, E.J., Greenland, L.P., and Ligon, D.T., Jr. (1972) Compositional data for twenty-one Fra Mauro lunar materials. Proceedings of the 3rd Lunar Science Conference, 2, 1215–1229.
Ryder, G. (1976) Lunar sample 15405: Remnant of a KREEP basalt-granite differentiated pluton. Earth and Planetary Science Letters, 29, 255–268.
——— (1985) Catalog of Apollo 15 Rocks. JSC Publication No. 20787, Curatorial Branch Publication 72, 1296 p. NASA Johnson Space Center, Houston.
——— (2002) Mass flux in the ancient Earth-Moon system and benign implications for the origin of life on Earth. Journal of Geophysical Research, 107, 5022, DOI: 10.1029/2001JE001583.
Ryder, G. and Norman, M.D. (1980) Catalog of Apollo 16 Rocks. JSC Publication No. 16904, Curatorial Branch Publication 52, 1144 p. NASA Johnson Space Center, Houston.
Ryder, G. and Schuraytz, B. (2001) Chemical variations of the large Apollo 15 olivine-normative mare basalt rock samples. Journal of Geophysical Research, 106, 1435–1451.
Shervais, J.W., Taylor, L.A., and Lindstrom, M.M. (1985) Apollo 14 mare basalts: Petrology and geochemistry of clasts from consortium breccia 14321.

Proceedings of the 15th Lunar Science Conference, in Journal of Geophysical Research, 90, C375–C395.

——— (1988) Olivine vitrophyres: A nonpristine high-Mg component in lunar breccia 14321. Proceedings of the 18th Lunar Science Conference, 45–57.

Shih, C.-Y. and Nyquist, L.E. (1989a) Isotopic and chemical constraints on models of aluminous mare basalts genesis. Lunar and Planetary Science, XX, 1002–1003 (abstract). Lunar and Planetary Institute, Houston.

——— (1989b) Isotopic constraints on the petrogenesis of Apollo 14 igneous rocks. In G.J. Taylor and P.H. Warren, Eds., Workshop on Moon in Transition: Apollo 14, KREEP, and Evolved Lunar Rocks, p. 128–136. LPI Technical Report, 89-03, Lunar and Planetary Institute, Houston.

Snyder, G.A. and Taylor, L.A. (2000) Impact processes and isotopic closure on planetary bodies and the Moon. Lunar and Planetary Science, XXXI, abstract 1220 (CD-ROM). Lunar and Planetary Institute, Houston.

——— (2001) Oldest mare basalts or impact melts? The role of differential melting of plagioclase in Apollo 14 high-Al basalts (abstract). Meteoritics and Planetary Science, 36, A194.

Snyder, G.A., Taylor, L.A., and Neal, C.R. (1992) A chemical model for generating the sources of mare basalts: Combined equilibrium and fractional crystallization of the lunar magmasphere. Geochimica et Cosmochimica Acta, 56, 3809–3823.

Snyder, G.A., Borg, L.E., Nyquist, L.E., and Taylor, L.A. (2000) Chronology and isotopic constraints on lunar evolution. In R.M. Canup and K. Righter, Eds., Origin of Earth and Moon, p. 361–395. Lunar and Planetary Institute, Houston.

Sun, S.-S. and McDonough, W.F. (1989) Chemical and isotopic systematics of oceanic basalts: Implications for mantle composition and processes. In A.D. Saunders and M.J. Norry, Eds., Magmatism in the Ocean Basins, Special Publication 42, p. 313–345. Geological Society of London.

Taylor, L.A., Shervais, J., Hunter, R., Shih, C.-Y., Bansal, B.M., Wooden, J., Nyquist, L.E., and Laul, J.C. (1983) Pre-4.2 AE mare basalt volcanism in the lunar highlands. Earth and Planetary Science Letters, 66, 33–47.

Taylor, S.R., Kaye, M., Muir, P., Nance, W., Rudowski, R., and Ware, N. (1972) Composition of the lunar uplands: Chemistry of Apollo 14 samples from Fra Mauro. Proceedings of the 3rd Lunar Science Conference, 2, 1231–1249.

Vaniman, D.T. and Papike, J.J. (1980) Lunar highland melt rocks; chemistry, petrology and silicate mineralogy. In Proceedings of the Conference on the Lunar Highlands Crust, p. 271–337. Pergamon Press, New York.

Walker, D., Longhi, J., and Hays, F. (1972) Experimental petrology and origin of Fra Mauro rocks and soil. Proceedings of the 3rd Lunar Science Conference, 2, 797–817.

Warner, R.D., Taylor, G., Keil, K., Ma, M.-S., and Schmitt, R. (1980) Aluminous mare basalts: New data from Apollo 14 course fines. Proceedings of the 11th Lunar Science Conference, 87–104.

Warren, P.H (1988) The origin of pristine KREEP: Effects of mixing between urKREEP and the magmas parental to the mg-rich cumulates. Proceedings of the 18th Lunar Science Conference, 233–241.

Warren, P.H. and Wasson, J.T. (1978) Compositional-petrographic investigation of pristine nonmare rocks. Proceedings of the 9th Lunar Science Conference, 1, 185–217.

——— (1979) The origin of KREEP. Reviews of Geophysics and Space Physics, 17, 73–88.

Warren, P.H., Afiattalab, F., and Wasson, J.T. (1978) Investigation of unusual KREEPy samples: Prostine rock 15386, Cone Crater soil fragments 14143, and 12023, a typical Apollo 12 soil. Proceedings of the 9th Lunar Science Conference, 1, 653–660.

Warren, P.H., Taylor, G.J., Keil, K., Shirley, D.N., and Wasson, J.T. (1983) Petrology and chemistry of two "large" granite clasts from the Moon. Earth and Planetary Science Letters, 64, 175–185.

Warren, P.H, Kallemeyn, G., and Kyte, F. (1997) Siderophile element evidence indicates that Apollo 14 high-Al mare basalts are not impact melts. Lunar and Planetary Science, XXVIII, 1501–1502 (abstract). Lunar and Planetary Institute, Houston.

Wiesmann, H. and Hubbard N. (1975) A compilation of the lunar sample data generated by the Gast, Nyquist, and Hubbard lunar sample PI-ships. Unpublished JSC document.

Wilhelms, D. (1987) The Geologic History of the Moon. U.S. Geological Survey Professional Paper 1348. U.S. Geological Survey, Washington, D.C.

Willis, J.P., Erlank, A.J., Gurney, J.J., Theil, R.H., and Ahrens, L.H. (1972) Major, minor, and trace element data for some Apollo 11, 12, 14, and 15 samples. Proceedings of the 3rd Lunar Science Conference, 2, 1269–1273.

Wilson, S.A. (1998) Data compilation for USGS reference material BHVO-2, Hawaiian basalt. U.S. Geological Survey, Open File Report. Available on-line at: http://minerals.cr.usgs.gov/geo_chem_stand/basaltbhv02.html.

MANUSCRIPT RECEIVED NOVEMBER 10, 2005
MANUSCRIPT ACCEPTED MAY 1, 2006
MANUSCRIPT HANDLED BY C. SHEARER